Molecular Structure of

$(Ga_2S_3)_x(GeS_2)_{1-x}$ Glasses by Raman Scattering

and T-modulated DSC

Liuchun Cai

2003

Department of Electrical and Computer Engineering and Computer Science

College of Engineering
University of Cincinnati

UNIVERSITY OF CINCINNATI

_____ , 20 _____

I,_____,
hereby submit this as part of the requirements for the
degree of:

_____

in:

_____

It is entitled:

_____ 2 3 x   2 1-x _____

_____

_____

_____

Approved by:

_____

_____

_____

_____

_____

Molecular Structure of $(Ga_2S_3)_x(GeS_2)_{1-x}$ glasses by Raman Scattering and T-modulated DSC

A thesis submitted to the

Division of Research and Advanced Studies
of the University of Cincinnati

In partial fulfillment of the
requirements for the degree of

MASTER OF SCIENCE

In the Department of Electrical & Computer
Engineering and Computer Sciences

2003

by

Liuchun Cai

Committee Chair: Prof. Punit Boolchand

ABSTRACT

The doping behavior of the group III additive Indium in Ge_xSe_{1-x} glasses is examined in temperature modulated DSC (MDSC) measurements. The results show that variation in T_g, $(dT_g/dy)_{obs}$, in $Ge_xIn_ySe_{1-x-y}$ glasses, in the floppy ($x = 0.10$), intermediate ($x = 0.22$) and stressed rigid ($x > 0.26$) phases reveal slopes that can be quantatively understood in term of a model in which In segregates into nanocrystalline In_2Se_3 clusters. A parallel behavior is suggested for Ga in stressed rigid ($x > 0.26$) base glasses.

Molecular structure of Ge_xS_{1-x} glasses in the $0.30 < x < 0.34$ range is examined by Raman scattering, [119]Sn Mössbauer spectroscopy, and MDSC. The results show that the stoichiometric glass, $x = 1/3$ ($T_g = 508°C$) is *partially polymerized* into 3 phases; a majority phase consist of $Ge(S_{1/2})_4$ tetrahedra (A); a Ge-rich minority phase consisting of ethanelike $Ge_2(S_{1/2})_6$ units (B), and a minority GeS phase consisting of distorted rocksalt $Ge(S_{1/6})_6$ units (C) in approximately 93.4 : 3.6 : 3.0 ratio as deduced from Raman scattering.

Raman Scattering and MDSC investigations of the molecular structure of $(GeS_2)_{1-x}(Ga_2S_3)_x$ glasses shows the existence of a rather striking anomaly when $x = 17\%$. In the $0 < x < 17\%$ range, additive (Ga_2S_3) enters the base glass as $Ga(S_{1/2})_4$ units forming part of the base glass network, and results in a Ge-rich Ge_2S_3 nanophase to segregate from the backbone. At $x > 17\%$, the additive (Ga_2S_3) now nucleates a Ga-rich, GaS like phase, releasing S that permits Ge_2S_3 nanophase to alloy back in the base glass network.

ACKNOWLEDGMENTS

I wish to express my deepest gratitude to professor Punit Boolchand for his guidance, advice, and support throughout my study as a graduate student at University of Cincinnati.

I appreciate help of professor M. Cahay, professor K. Roenker and professor B. Goodman for their expertise and assistance as member of my thesis committee.

My appreciation goes to my colleague friend Dr. Wayne Bresser who helped me with my Al-Te work at Northern Kentucky University. Thanks are due to Dr. Sergey Mamedov, Mr. Daniel Georgiev, Mr. Tao Qu, Ms. Fei Wang, Mr. Swapnajit Chakravarty and Mr. Ping Chen for their company in the laboratory and at the conferences we attended. I would like to thank Mr. Donovan Pena, Mr. Bo Sun from Materials and Chemical Engineering department for their help in photobleaching experiment. My thanks also go to my colleagues and departmental staff at ECECS department for their assistance and friendship.

Finally a very special thanks to my wife Emily Han and my family for their love, encouragement, help and sacrifice which made this work possible.

TABLE OF CONTENTS

LIST OF FIGURES

Chapter 1

Chapter 2

Chapter 3

Chapter 4

Chapter 1

INTRODUCTION

Glasses have often been described as *random networks* for the past 30 years [1]. There are several reasons. The standard description of glasses as random networks can be modeled for molecular dynamic studies on computers [2]. Aspects of average structure as established by diffraction methods can be compared to predictions of such models.

Often good agreement has been claimed to justify structure of glasses to consist of random networks. However, this does not mean that glasses possess a truly *random character*. Diffraction measurements provide an average global view. Extracting details of glass structure from such measurements is difficult because of the *averaging* intrinsic to these measurements. In fact, recent experiments utilizing *local probes* such as Raman scattering, Mӧssbauer spectroscopy, NMR and a thermal method- temperature modulated DSC have revealed [3] that it is rare that glasses are made of strictly *random* networks. Although SiO_2 is often cited as a good example of a random network , recent experiments reveal that this may not be the case. One of the best examples of a random network is the $Ge_{1/4}S_{7/12}I_{1/6}$ ternary chalcohalide in which iodine *randomly* scissions the S bridges to produce a random network as recently discussed by Y.Wang et al [4].

Recently, profound progress in understanding glass structure has emerged from measuring their elastic response [5] using a local probe like Raman scattering. Experiments performed as a function of global connectivity or mean coordination

number, **r**, have shown that there are in general 3 distinct elastic phases, *floppy*, *intermediate* and *stressed-rigid*. These phases have now been observed in As-Se [6], As-Ge-Se [7], Ge-Se [8,14], P-Se [9], P-Ge-Se [10] glasses. In fig. 1.1 below we reproduce results on the binary Ge-Se glasses taken from ref. [14]. Here one finds the non-reversing relaxation enthalpy at the glass transition , $\Delta H_{nr}(r)$, shows a global minimum in the 2.4 < r < 2.52 range.
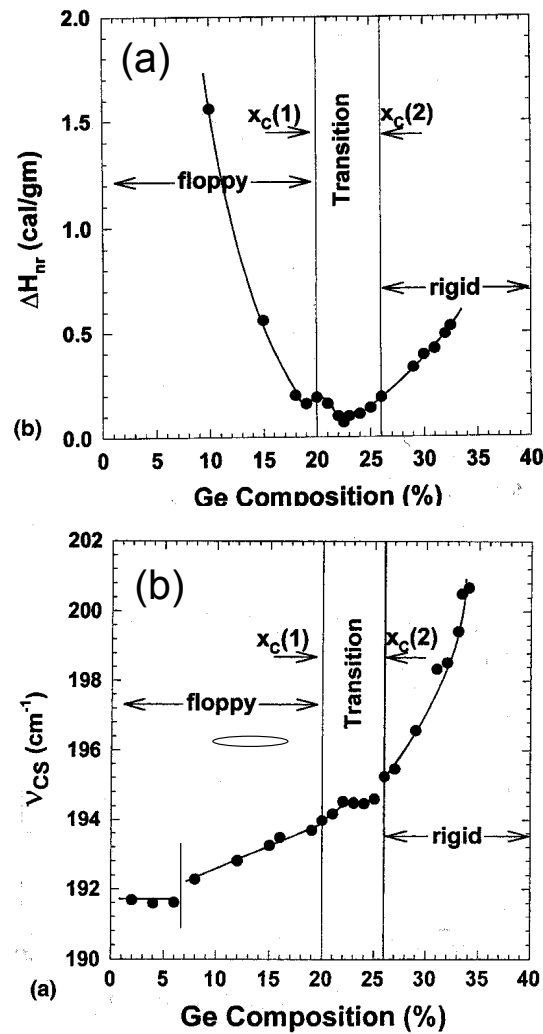
Figure 1.1 (a) Non-reversing heat-flow, $\Delta H_{nr}(r)$, variation in Ge-Se glasses taken from [14]. (b) Corner-sharing mode frequency variation, $\upsilon_{cs}(x)$, in Ge_xSe_{1-x} glasses from Macro-Racro measurements taken from ref. [14].

The optical elasticity of these glasses has been studied in macro-Raman studies [8]. One finds that the frequency squared of the corner-sharing $Ge(Se_{1/2})_4$ tetrahedra to display distinct kinks with well defined power-laws in different ranges. These results are signatures of *three* distinct elastic phases in these glasses; Se-rich glass compositions (0 < x < 0.20) consisting of Se_n-chain fragments are *floppy,* glass compositions in the 0.20 < x < 0.25 are *isostatically rigid*, and those in the 0.26 < x < 1/3 range are *stressed-rigid*.

1.1 Group III Additives in Chalcogenide Glasses

The local and medium range structures of Group III additives, such as Ga and In, in base chalcogenide glasses continues to be poorly understood subject [10-11]. The nature of local structures (pyramids or tetrahedra) and medium range structures (n-membered rings, as local structures incorporated in the base glass network) remain open questions.

In this work, I have examined the alloying behavior of indium additive in base Ge_xSe_{1-x} glasses. I have examined ternary glasses of the type, $Ge_xIn_ySe_{1-x-y}$, in the additive concentration 0 < y < 0.10 range at x = 0.10 (floppy), x= 0.22 (rigid) and x = 0.26 *stressed rigid.* Raman scattering and MDSC experiments were undertaken. In the latter measurements of $T_g(x,y)$ were measured, and the slopes dT_g/dy were established. These results are analyzed by Stochastic Agglomeration theory [12-13]. The results show that In as an additive in stressed rigid glasses, in general, nanoscale phase separates. In floppy and rigid glasses, a similar alloying behavior is suggested. In all cases In_2Se_3-rich clusters segregate from the base glasses. These results suggest that the alloying behavior

of this oversized additive in base chalcogenide glasses is the same. In general, this does not have to be the case.

1.2 Nanoscale Phase Separation of GeS$_2$ Stoichiometric Glass

The second phase of my work is to examine the processing conditions sufficient to synthesize *homogeneous* bulk binary Ge-S glasses. Often the problem in the past has been to identify experimental probes that would permit one to distinguish homogeneous from inhomogeneous glasses by *virtue of synthesis* or incomplete alloying. Here we have used Raman scattering and MDSC to show that, in general, reaction times in excess of 48 hours are needed to homogeneously alloy elemental Ge with S at 930ºC. It is important to establish these conditions in glass science research because many of the physical properties of these glasses published to date could arise from sample inhomogeneities that are strictly a consequence of *incomplete reaction times* in the alloying process. On the other hand, inhomogeneities in glass structure could be *intrinsic* i.e. due to nanoscale [14] or macroscale [15] phase separation of the glasses. Our experiments reveal that binary Ge$_x$S$_{1-x}$ glasses at x > 0.31 intrinsically *nanoscale phase separate* [16] into S-rich and Ge-rich regions.

1.3 Molecular Structure of (Ga$_2$S$_3$)$_x$(GeS$_2$)$_{1-x}$ Glasses

The third phase of my work is to examine the molecular structure of ternary (Ga$_2$S$_3$)$_x$(GeS$_2$)$_{1-x}$ glasses. The ternary has attracted widespread interest as a host for light

emission studies using rare-earth additives [17]. Experiments reveal rare-earth additives to be homogeneously distributed in these base glasses [18] and the photoluminescent efficiencies to be rather high, although the molecular origin for the behavior remains an open issue. It is likely that trivalent rare-earth additives replace Ga^{3+} cations in the prevailing nanophases of the base glasses. And it remains to be understood what Ga-based nanophase exists in these glasses. During the course of this work, we discover the existence of a rather striking anomaly near x = 17% in this ternary. Such glasses are dark in color, while those at x < or > 17% are yellow in color. Fig. 1.2 shows the color of the samples synthesized in the present work.

It appears that Ga_2S_3 enters GeS_2 base glass largely as a tetrahedral $Ga(S_{1/2})_4$ local units in the $Ge(S_{1/2})_4$ backbone in the 0 < x < 17% region. At higher x (> 17%), a nano-crystalline Ga-rich phase based on the GaS structure nucleates. Formation of the latter phase makes S available and redissolves the Ge_2S_3 phase with the GeS_2 phase, and drives the glass sample yellow in color.
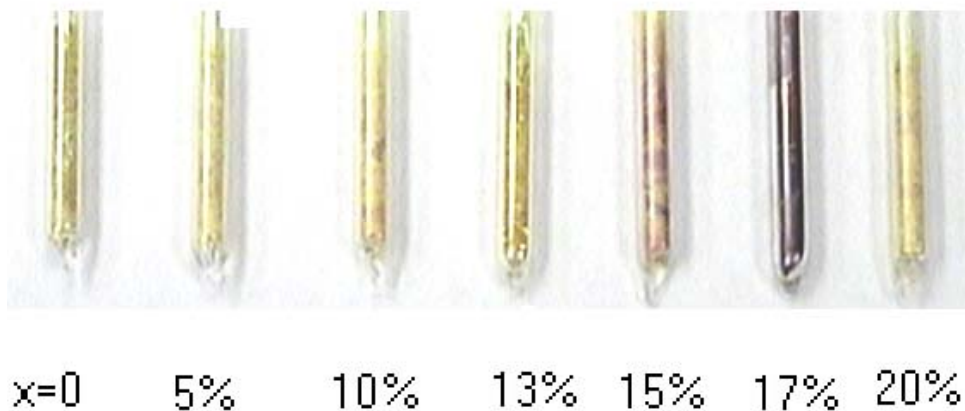
Figure 1.2 The color of $(GeS_2)_{1-x}(Ga_2S_3)_x$ samples

11

In summary, group III additives of Ga and In display a *rich variety* of *local* and *medium range* structures in base chalcogenide glasses. In our work the alloying behavior appears to be controlled by additive size and network stress. The latter varies in a systematic fashion as a function of mean coordination number r, and is a global minimum in the isostatically rigid or intermediate phase.

The thesis is organized as follows: Chapter 2 provides the experimental procedures including the sample synthesis, details of thermal measurements, Raman Scattering and Mössbauer spectroscopy. Chapter 3 presents the experimental results. Chapter 4 is devoted to detailed discussion of specific issues outlined above. The principal conclusions of this work are summarized in chapter 5.

REFERENCES:

1. M. F. Thorpe, in *Insulating and Semiconducting Glasses*, Ed.   P.Boolchand, (World Scientific Press,Inc 2000), P. 96.

2. D.A. Drabold, in *Insulating and Semiconducting Glasses*, Ed. P.Boolchand, (World Scientific Press,Inc 2000), P. 607.

3. P.Boolchand, *in Insulating and Semiconducting Glasses*, Ed. P.Boolchand, (World Scientific Press,Inc 2000), p. 369.

4. Y.Wang, J.Wells, D.G.Georgiev**,** P. Boolchand, Koblar Jackson, M. Micoulaut, Phys. Rev. Lett**. 87** (2001), 5503.

5. H. He and M.F. Thorpe, Phy. Rev. Lett. **54** (1985), 2107.

6. D.G. Georgiev, P.Boolchand, M. Micoulaut, Phys. Rev. B **62** (2000), 9268.

7. Tao Qu, D,G,Georgiev, P.Boolchand, M.Micoulaut, Mater. Res. Soc. Symp. Proc. 754 (2003) (in press).

8. D.G. Georgiev, M. Mitkova, P.Boolchand, G. Brunklaus, H. Eckert, M. Micoulaut, Phys. Rev. B **64** (2001), 4204.

9. S. Chakravarty, D.G. Georgiev, P.Boolchand (unpublished).

10. A. Giridhar, S. Mahadevan, J. Non.Cryst. Solids **126** (1990), 161.

11. S. Mahadevan, A. Giridhar, J. Non.Cryst. Solids **152** (1993), 42.

12. K.A. Jackson, A. Briley, S. Grossman, D.V. Porezag, M.R. Pederson, Phys. Rev. B **60** (1999), R14985.

13. C. Massobrio, A. Pasquerello, R. Car, Phys. Rev. B **64** (2001), 144205.

14. P. Boolchand, X. Feng, W.J. Bresser, J.Non-Cryst. Solids **293** (2001), 348.

15. P.Boolchand and W.J.Bresser, Nature **410** (2001),1070.

16. Liuchun Cai and P. Boolchand, Phil. Mag. B **82** (2002),1649.

17. R.S. Quimby and B.G. Aitken, J. Non. Cryst. Solids **320** (2003),100.

18. B.G. Aitken, C.W. Ponader, R.S. Quimby, C. R. Chimie **5** (2003),1.

Chapter 2

EXPERIMENTAL PROCEDURE

In this chapter, we provide details on sample preparation and experimental procedure used to characterize the samples. The methods include Modulated Differential Scanning Calorimetry (MDSC), Raman Scattering and Mössbauer Spectroscopy. Results will be discussed in chapters 3 and 4.

2.1 Sample Synthesis

Binary Ge_xS_{1-x} glasses in the 30% < x < 34% interval, ternary $(Ga_2S_3)_x(GeS_2)_{1-x}$ in the 0<x< 55% internal and ternary $In_yGe_xSe_{1-x-y}$ in the 0 < y < 0.10, 0.10 < x <1/3 interval were synthesized by reacting 99.999% In, Ge, S, Se and Ga pieces from Cerac, Inc.. The starting materials were sealed in evacuated (5 x 10^{-7} Torr) fused quartz tubings of 5 mm id and 1 mm wall thickness. Typical sample size was 2 grams. The phase diagrams of Ge-S [1], and Ga-Ge-S [2] are shown in Figure 2.1 and Figure 2.2, respectively.

The temperature was slowly (over 2 days) increased to 1000°C, and melts homogenized at that temperature for at least t_h = 72 hours before lowering temperatures to a suitable quench temperature, $T_q = T_l + 30°C$, and equilibrating melts for t_e = 24 hours before a quench in cold water. Care was taken to insure that the T_q did not exceed

T_l(liquids) by more than 30°C, otherwise inner walls of sample tubes develop a yellow flashing suggestive of a S-rich deposit.
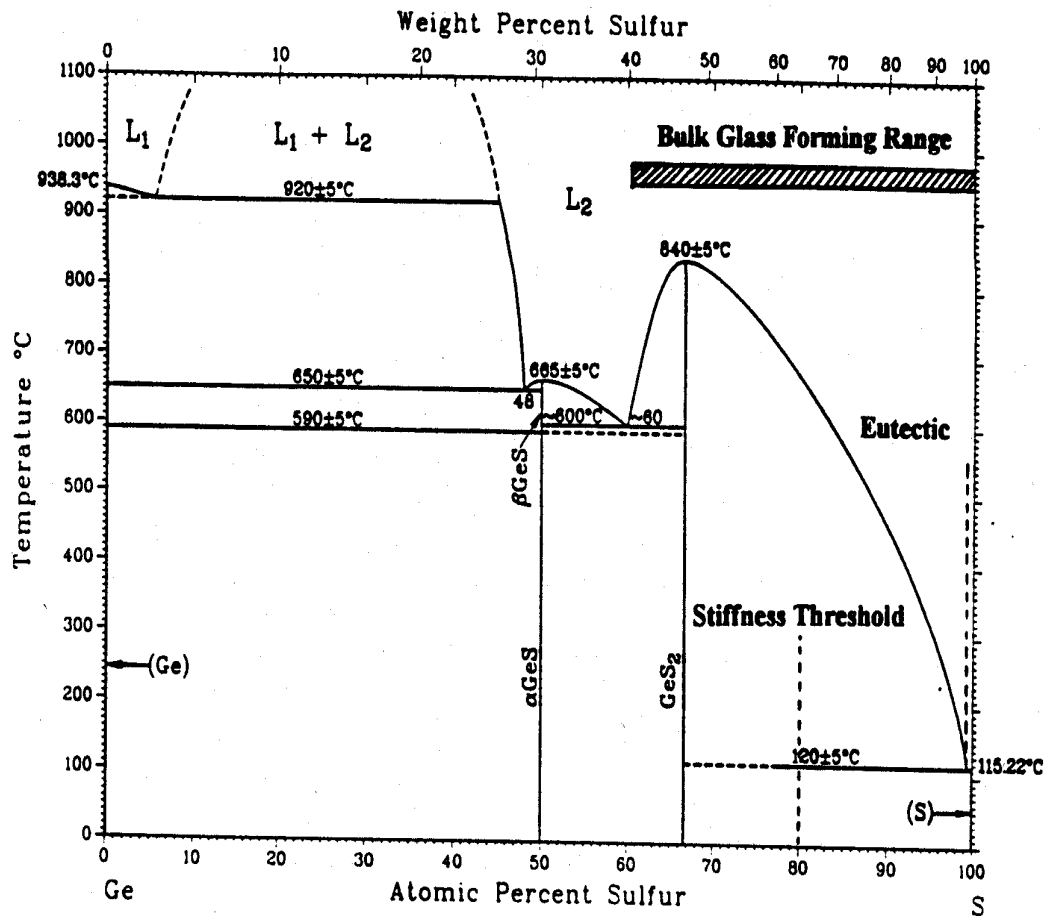
Figure 2.1 Phase diagram of Ge-S system taken from [1].
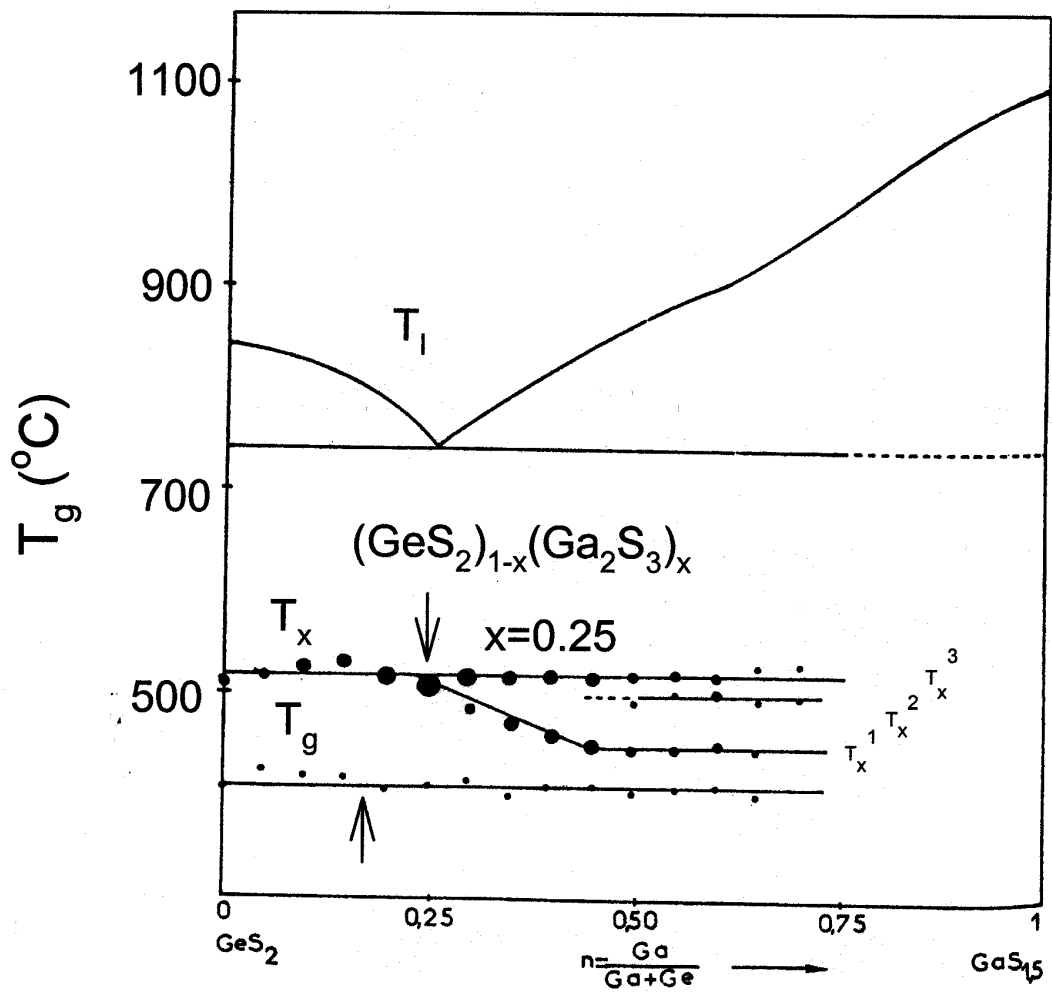
Figure 2.2 Phase of diagram of Ga-Ge-S system taken from Loireau-Lozac'h and Guittard. In this earlier study samples were studied at 5 molar % step increase in Ga concentration starting from GeS_2. The up-arrow indicates the concentration where in a global minimum in T_g is observed in the present work. The T_g reported in ref.2 is found to be about 250^oC. Multiple crystallization temperatures (T_x^1, T_x^2, T_x^3) are observed at x >1/4.

Samples homogenized at 1000°C for a shorter period such as t_h = 24 hours, were found to display fluctuations in T_gs of up to 25°C from one part of the sample to the other. These were found to correlate well with micro-Raman estimates of sample stoichiometry. These T_g fluctuations examined at x = 31.6% in the Ge_xS_{1-x} binary glass system, translate into compositional fluctuations in x of typically about 1.0 at.%. Upon increasing t_h to 72 hours or more, fluctuations in T_g s decreased to 2°C as glass samples became homogeneous. These results will be discussed in chapter 3.

2.2 Raman Scattering

The Raman effect results from the interaction of vibrational and/or rotational motions of molecules with the electromagnetic radiation. The Quantum mechanical mode is following: A molecular motion can have only certain discrete energy state. A change in state is thus accompanied by the gain or loss of one or more quanta of energy. Scattering processes involve at least low quanta acting simultaneously in the light matter system. Simple elastic scattering occurs when a quantum of electromagnetic energy is created at the same time that an identical one is annihilated. Thus, the molecule is unchanged by the event. In Raman effect (this is inelastic process), the two photons are not identical and there is a net change in the state of the molecule. If the created photon is less energetic than the annihilated one, the scattered light is observed at a frequency that is lower than that of the incident light. This is referred to As Stokes Raman Scattering. On the other hand, if the created photon is the more energetic of the two, the Raman frequency will be higher than that of the laser and the anti-Stokes spectrum will be produced [3-4].
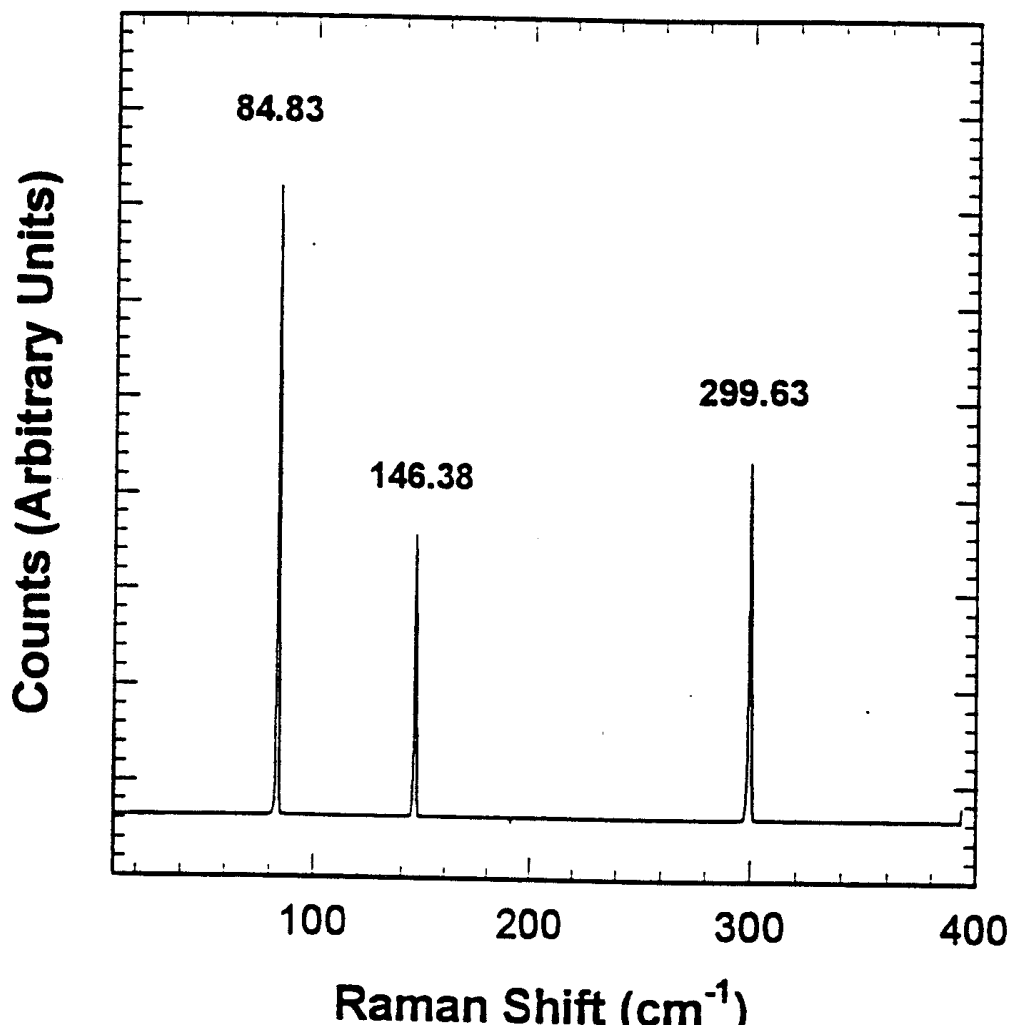
Figure 2.3 Raman Scattering calibration using Neon discharge lamp. There are three sharp peaks at 84.83 cm^{-1}, 146.38cm^{-1} and 299.63cm^{-1} used to calibrate the CCD and monochrometer.

In glasses, the Raman vibrational modes are usually broadened compared to those in crystalline materials due to an intrinsic spread in bond angles and bond lengths of specific building blocks of the glassy network [3].

Our spectra of the glasses were recorded at room temperature using a model T64000 triple monochromer system from instrument S.A. equipped with a CCD detector and a microscope attachment. The magnification of the microscope objective was 80X, which yields a spatial resolution of 1-2 um. The back-scattered radiation was excited using 6mW of 514.5 nm from Ar-ion laser and the 647.1 nm from a Kr-ion laser in a conventional macro-Raman set up with glass samples contained in the quartz tubes used for synthesis.

The system was carefully adjusted to get the optimum performance before each measurement. After such adjustment, more than 800 counts/sec on a CCD detector can be obtained for c-Si sample on the 519.9 cm^{-1} phonon with only 6 mW laser power on the sample.

At the start of each run, the triple monochrometer system was calibrated using a Ne discharge lamp or c-Si sample. Ne discharge lamp revealed 3 atomic transitions at 84.38cm^{-1}, 146,38 cm^{-1} and 299.63 cm^{-1} in the CCD spectral window as shown in figure 2.3. The typical line-width of these lines was found to be 1.3cm^{-1}. The spectral window was kept unchanged throughout the measurements. In fact, the stability of the spectrometer system was tracked periodically by recording Ne spectra during the course of the Raman measurements. Typically the system was calibrated on the 299.63cm^{-1} line. The system was also calibrated by the sharp LO Raman scattering on the 519.9 cm^{-1} phonon for c-Si sample, which is shown figure 2.4.
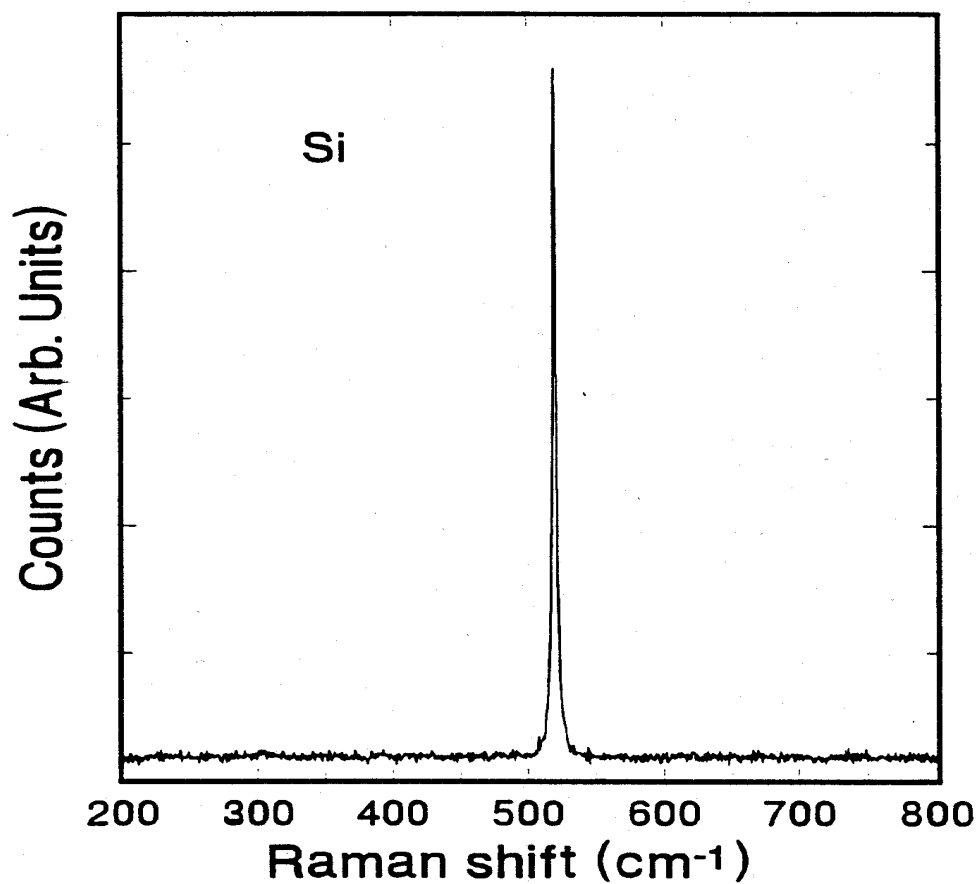
Figure 2.4 Raman spectra of crystal Si. The sharp Raman active phonon mode with the frequency of $519.8 cm^{-1}$ was chosen to calibrate the Raman system.

2.3 Modulated Differential Scanning Calorimetry (MDSC)

Since MDSC offers higher sensitivity, experiments can be done at much lower scan rates (typically 1 order of magnitude lower than in DSC), which minimizes scan-rate shifts [5-6]. By scanning up and then down in T across T_g, it is possible to eliminate scan-rate shifts to T_g. The method also permits a measurement of ΔH_{nr} *independent of* scan

rates. In MDSC, the heating profile consists of a sinusoidal modulation of a linear T-ramp. The amplitude of the modulated heat flow provides the response of the glass system that tracks the sinusoidal variation, and represents a direct measure of the reversing heat flow (H_r). The average value of the modulated heat flow yields total heat flow (H_t), a quantity that is usually measured in a DSC experiment (corresponding to no T-modulation). The arithmetic difference between H_t and H_r then yields the non-reversing heat flow (H_{nr}). The figure 2.5 shows the reversing, non-reversing and total heat flow signals from a stoichimetric GeS_2 glass.

Thermal analysis of our glass samples was performed using a Thermal Analyst 2920 MDSC system to characterize glass transition temperature T_g. In such type of measurements, typically about 10~20mg of a sample was encapsulated in an aluminum pan. Prior to measuring MDSC scans of samples, the heating cell baseline was calibrated. Temperature calibration of the heating cell was performed using Indium and Zinc standards and the heat capacity calibration was performed using a sapphire standard provided by TA Instruments [7].
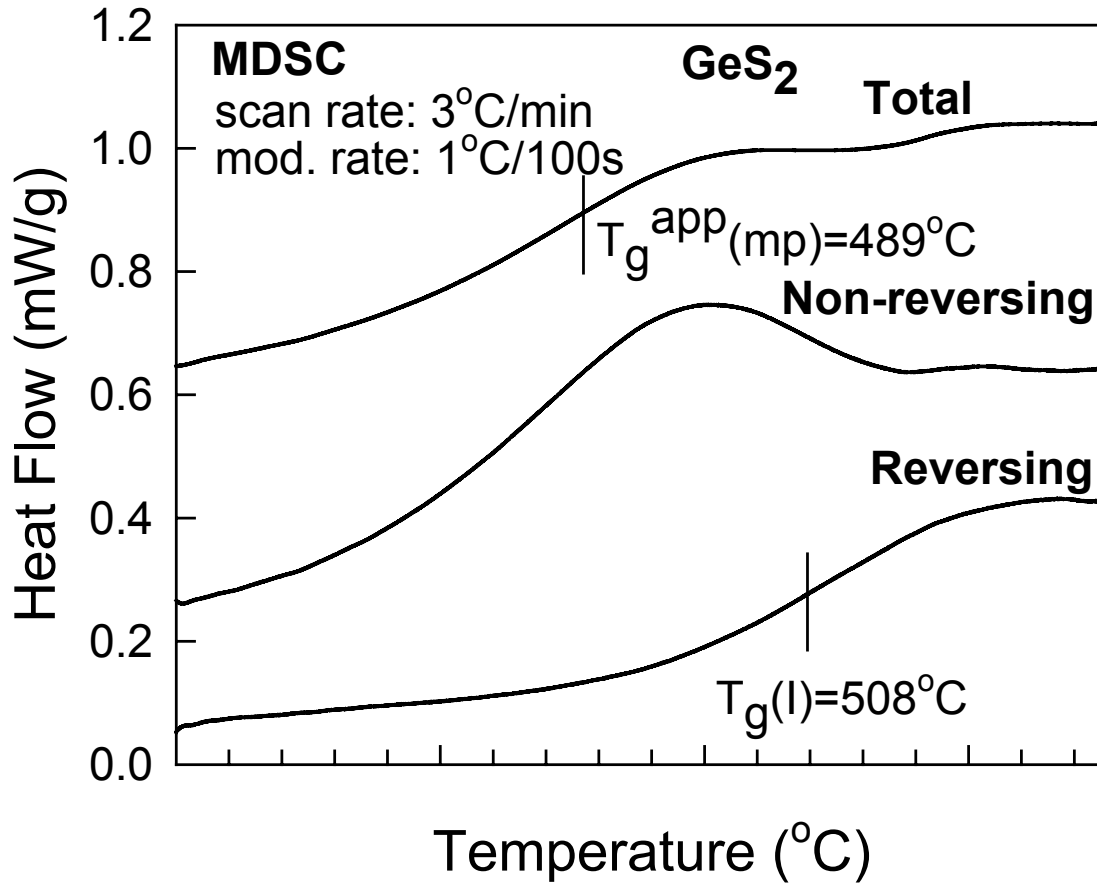
Figure 2.5 MDSC scan of GeS$_2$ glass sample. T$_g$, Reversing, non-reversing and total heat flow are all shown.

In a typical MDSC scan, the following were used as operating conditions. Scan rat was 3 ^{o}C pea minute, modulation amplitude 1 ^{o}C and a modulation period 100 seconds. The glass transition temperature T$_g$ is defined as the inflexion point of the endothermic step.

2.4 ^{119}Sn Mössbauer Absorption Spectroscopy

^{119}Sn Mössbauer absorption Spectra of glass samples were using obtained using a Ca^{119m}SnO$_3$ source developed in our laboratory. Both source and absorber were mounted onto a vertical Mössbauer drive and cooled done to LHe (LN$_2$) temperature. A Ge detector was used to cool with LN$_2$. (Ge$_{0.99}$Sn$_{0.01}$)$_x$S$_{1-x}$ and (Ge$_{0.99}$Sn$_{0.01}$S$_2$)$_{1-x}$(Ga$_2$S$_3$)$_x$ glasses doped with trace of enriched ^{119m}Sn were independently synthesized and examined as the absorber. . The system setup [8] we used is illustrated in figure 2.6. The data was stored in a multi channel analyzer using a PCAII card in a PC-486 computer.

We undertook two types of ^{119m}Sn measurements. One was performed at 77K for almost all the glasses. The other was undertaken at 4.2K for selected glass samples. In the 77K measurements, the complex spectra were fit to one site or multi-sites dependent upon sample type. We also studied the Mössbauer effect parameters such as quadrupole splitting (Δ) and isomer shift (δ) and Site Intensities (A : B : C). The figure 2.7 shows ^{119}Sn Spectrum of a (Ge$_{0.995}$Sn$_{0.005}$)$_{33}$S$_{67}$ glass sample taken at 4.2 K. (b) and (c) panel show deconvolution of the lineshqape into 3 sites (A, B and C) and 2 sites (A,B), respectively. Systematic misfits appear at the arrows location when 2 sites are used.
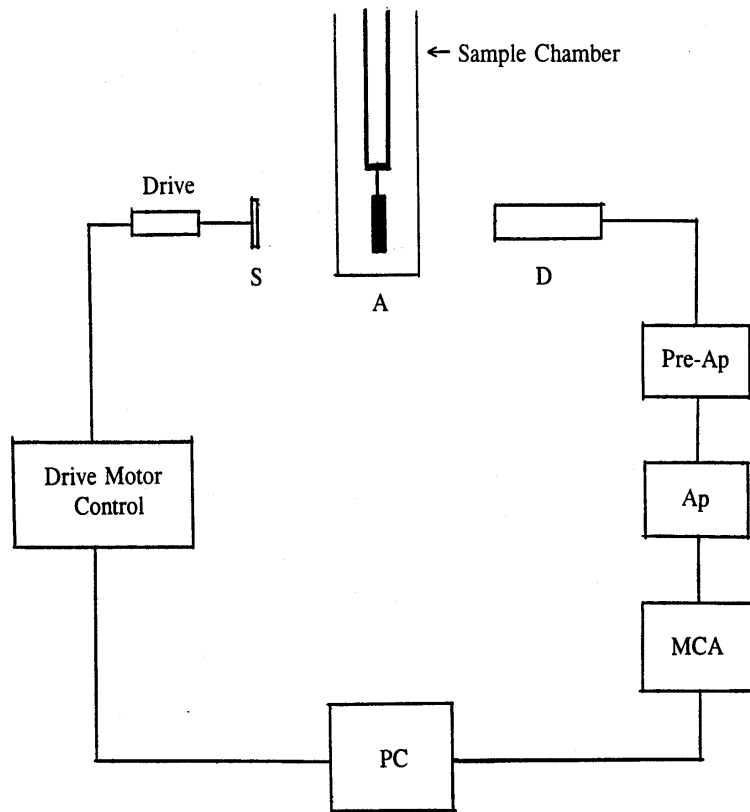
Figure 2.6 A block diagram of temperature controlled Mössbauer spectrometer used for our ^{119}Sn measurements. S = ^{119m}Sn Source, A = absorber (filled rectangle), D = detector, A_p = amplifier, MCA = multi-channel analyzer [8].
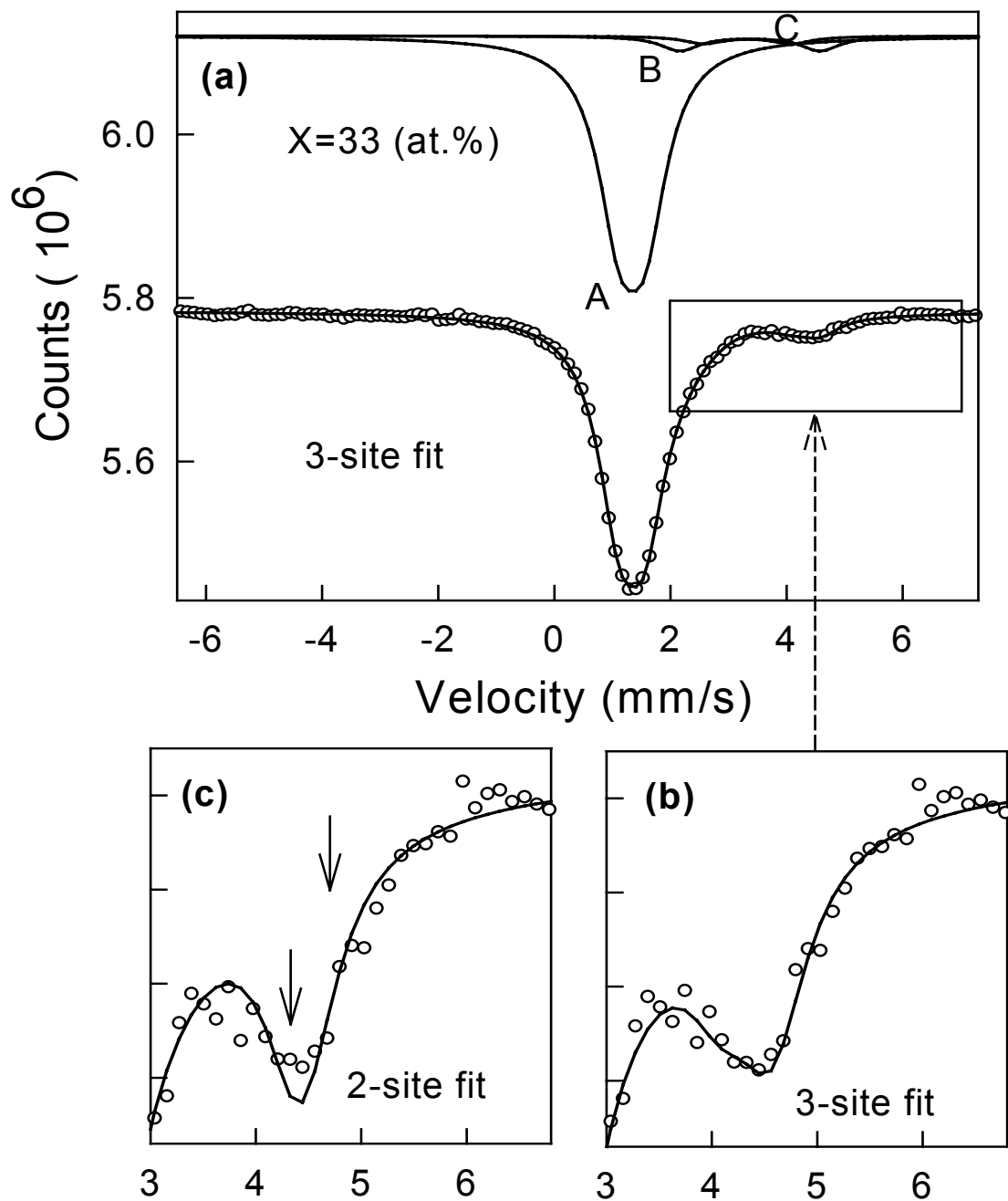
Figure 2.7 (a) ^{119}Sn Spectrum of a $(Ge_{0.995}Sn_{0.005})_{33}S_{67}$ glass sample taken at 4.2 K. (b) and (c) panel show deconvolution of the lineshqape into 3 sites (A, B and C) and 2 sites (A, B), respectively. Systematic misfits appear at the arrows location when 2 sites are used.

REFERENCES:

1. C. H. Liu, A. S. Pashinkin and A.V. Novoselova, Dokl. Aksf. Nauk SSSR, **151** (1963),1335.

2. A.M. Loireau-Lozac'h, and M. Guittard, Ann. Chim. **10** (1975),101.

3. G. Turrell and J. Corset, *Raman Microscopy: Developments and Applications*, Acdemic Press 1996, p1-25.

4. N.B.Colthup, L. H. Daly and S. E. Wiberley, *Introduction to infrared and Raman Spectroscopy*, Academic Press, InC, 1990,p1-75.

5. X. Feng, MS. Thesis, Univ. of Cincinnati, 1997 (unpublished).

6. D. Selvanathan M. Thesis, Univ. of Cincinnati, 1998 (unpublished).

7. TA Instruments, Modulated DSC^{TM} Compendium (1996).

8. M, Zhang Ph.D thesis, Univ. of Cincinnati, 1995(unpublished), p24.

Chapter 3

EXPERIMENTAL RESULTS

In this chapter, we provide the experimental results on (a) In doping effects in Ge_xSe_{1-x} glasses, (b) binary Ge_xS_{1-x} glasses in the $0.3 < x < 0.34$ range and (c) $(GeS_2)_{1-x}(Ga_2S_3)_x$ glasses. Raman Scattering, glass transition temperatures, ^{119}Sn Mössbauer spectroscopy results will be presented.

3.1 Indium as an Additive in Ge_xSe_{1-x} Glasses

We have examined In doping affects in Ge_xSe_{1-x} glasses. Figure 3.1 and figure 3.2 show the glass transition temperature, $T_g(y)$ and nonreversing heat flow, $\Delta H_{nr}(y)$ as a function of y in ternary $Ge_{10}In_ySe_{90-y}$ and $Ge_{22}In_ySe_{78-y}$ glasses, respectively. MDSC measurements were performed at the scanning rate and amplitude modulation rate of 3 ^{o}C/min and 1 ^{o}C/100sec, respectively. The results show that $T_g(y)$ of $Ge_{10}In_ySe_{90-y}$ glass to increase, and $\Delta H_{nr}(y)$ to decrease. For ternary $Ge_{22}In_ySe_{78-y}$ glasses, $T_g(y)$ and $\Delta H_{nr}(y)$ are found to increase. Nonreversing heat flow of $Ge_{22}In_ySe_{78-y}$ is similar to its T_g's. Of special interest here are the slopes of T_g, dT_g/dy that are plotted in insets of figure 3.1 (a) and figure 3.2 (a). The dT_g/dx variation in bases materials also shown in these insets. The slopes, dT_g/dy from DSC results on ternary $Ge_{10}Sb_ySe_{90-y}$, $Ge_{10}As_ySe_{90-y}$, $Ge_{20}Sb_ySe_{80-y}$ and $Ge_{20}As_ySe_{80-y}$ glasses taken from ref. [1] and [2] are displayed in Figure 3.3 and figure 3.4.
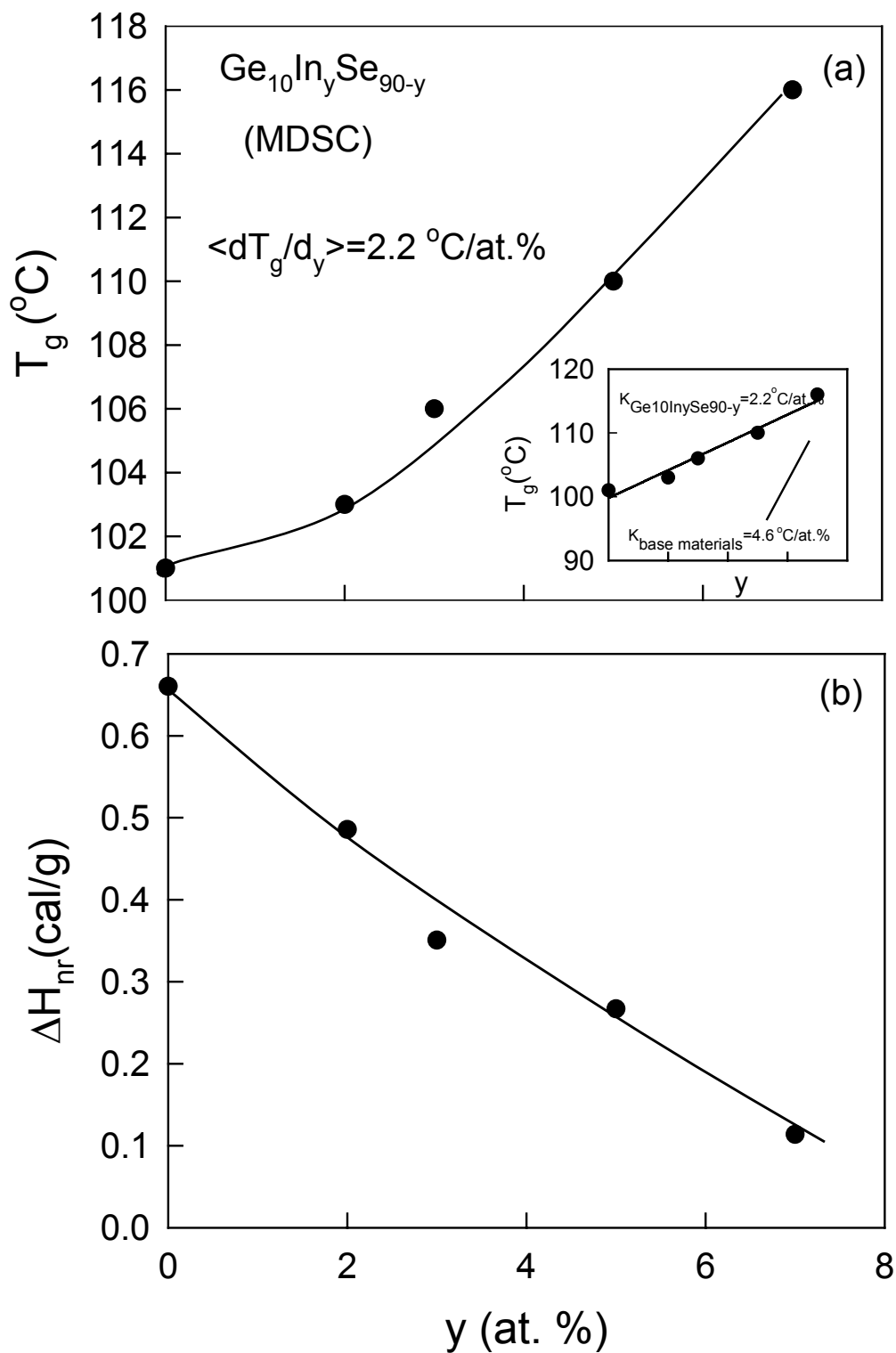
Figure 3. 1 T_g and ΔH_{nr} variation of MDSC as a function of y in $Ge_{10}In_ySe_{90-y}$ ternary glasses.
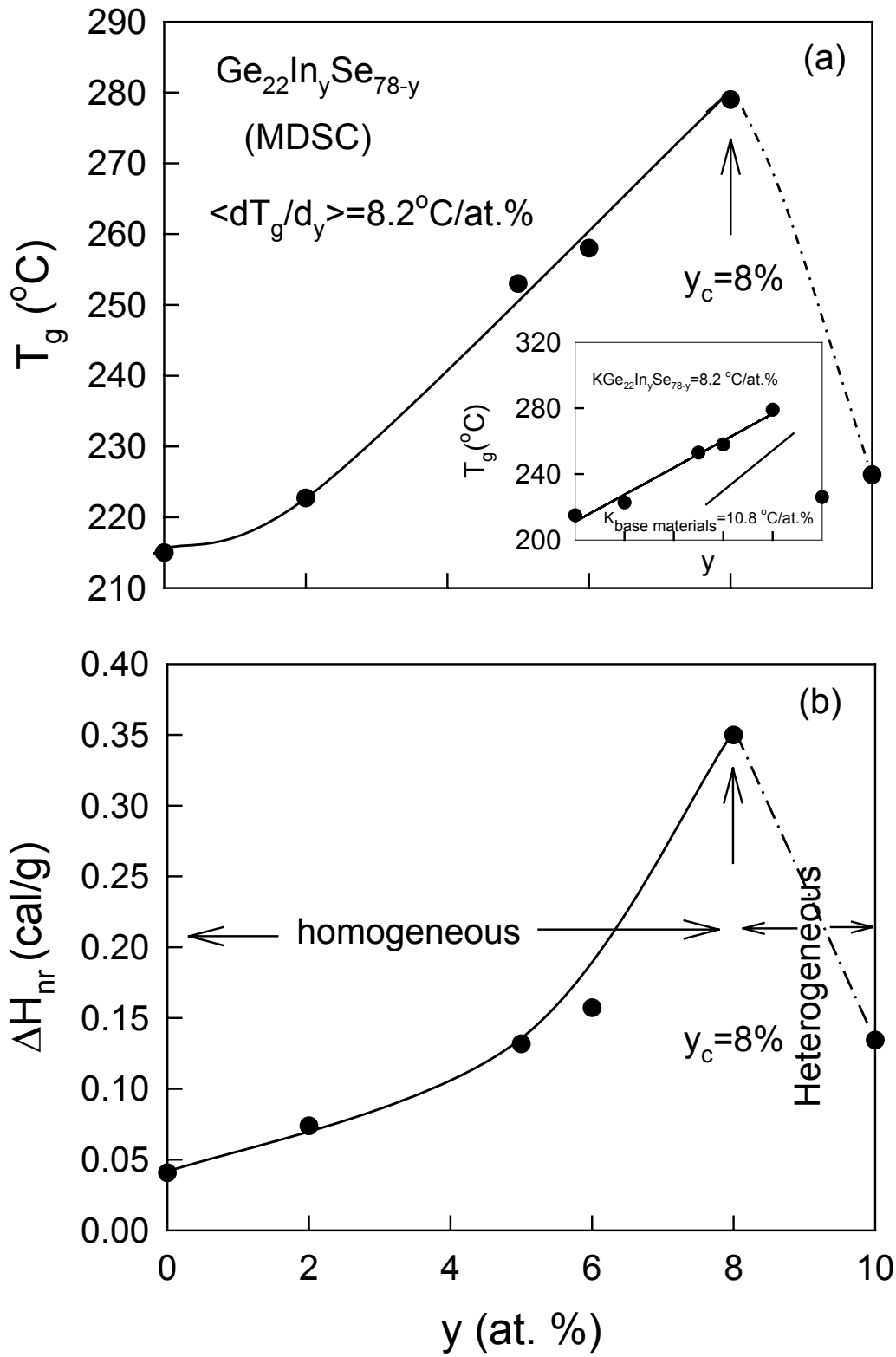
Figure 3.2 T_g and ΔH_{nr} variation of MDSC as a function of y in $Ge_{22}In_ySe_{78-y}$ ternary glasses.
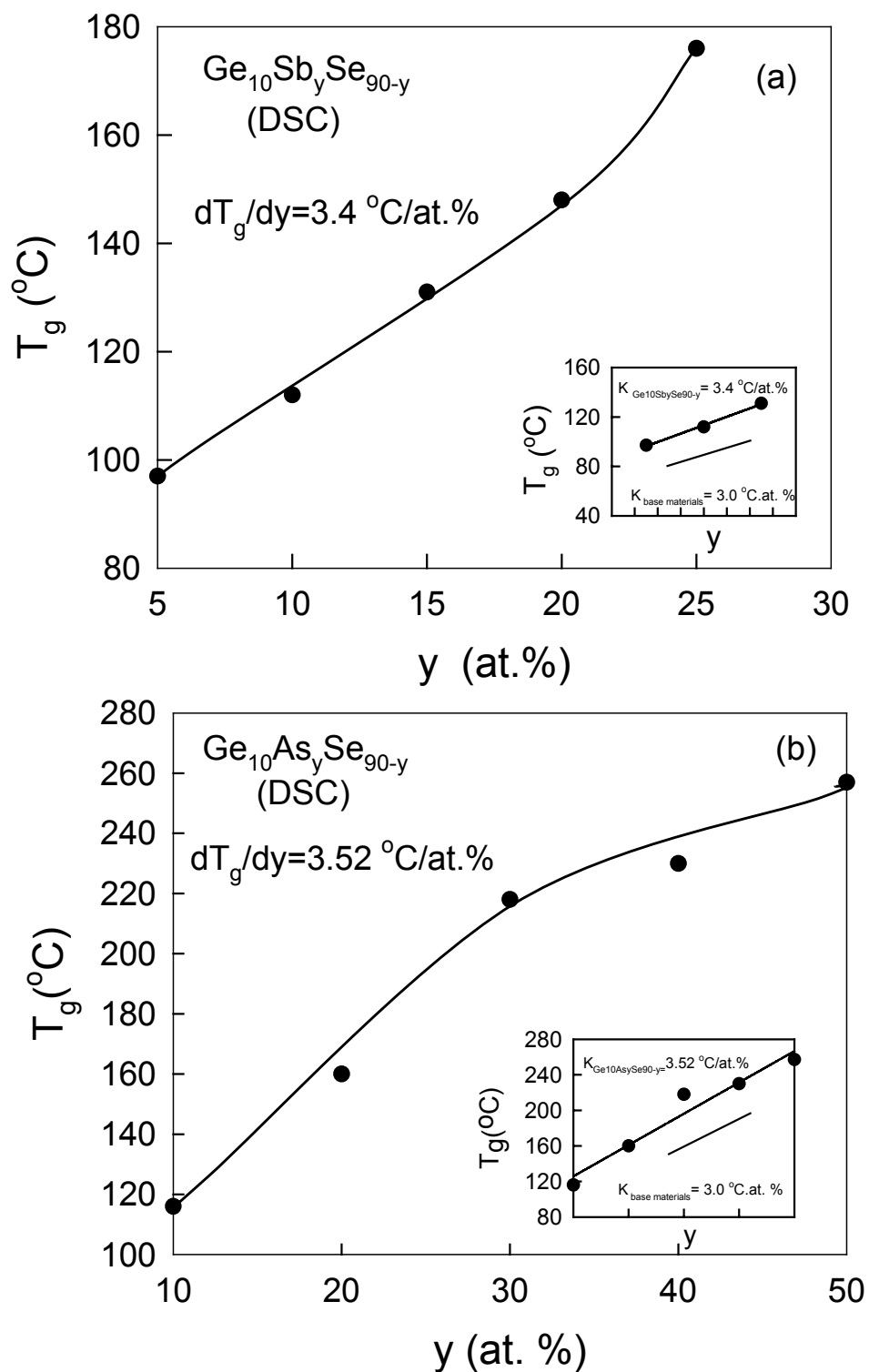
Figure 3.3 T_g variation of DSC as a function of y in $Ge_{10}Sb_ySe_{90-y}$ and $Ge_{10}As_ySe_{90-y}$ ternary glasses taken from ref. [1] and [2].
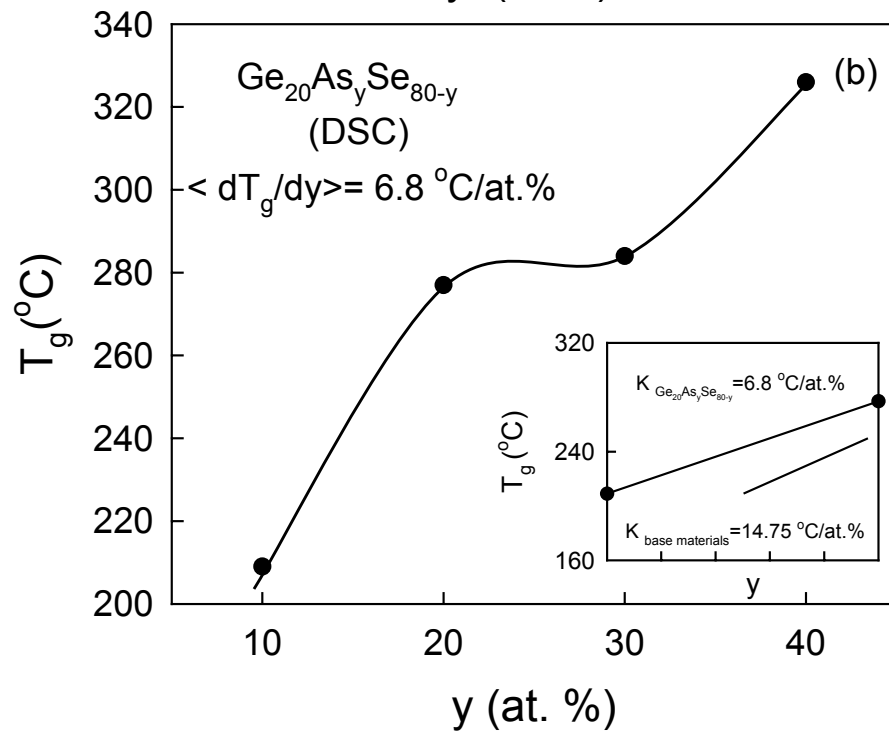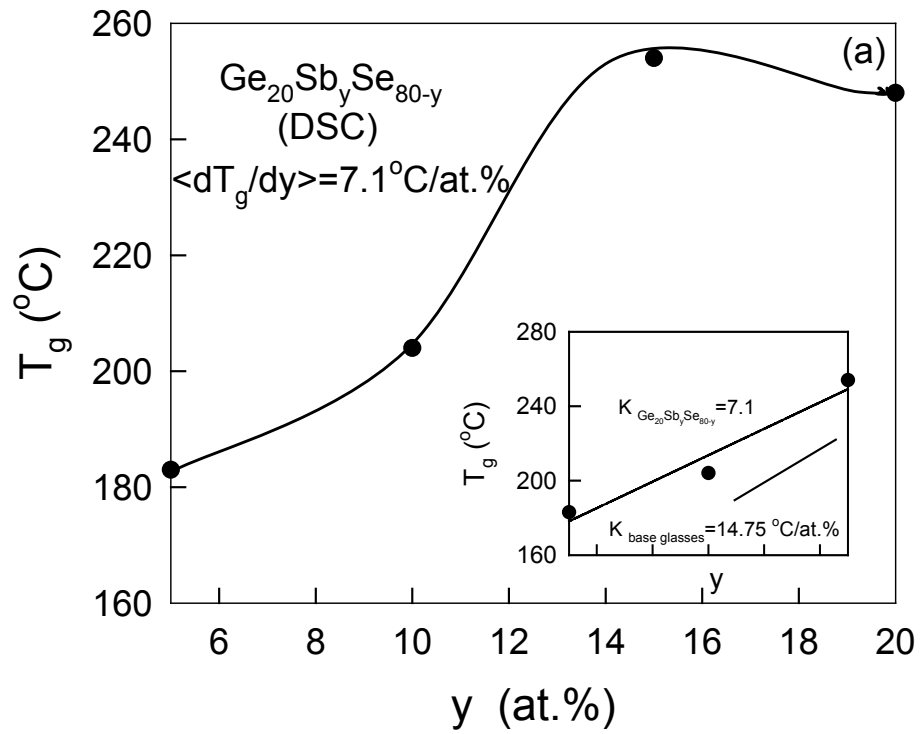
Figure 3.4 T_g variation of DSC as a function of y in $Ge_{20}Sb_ySe_{80-y}$ and $Ge_{20}As_ySe_{80-y}$ ternary glasses taken from ref.[1] and [2].

3.2 Molecular Structure of Binary Ge_xS_{1-x} Glasses

Recent interest in this binary glass comes from understanding the molecular structure of these glasses and particularly the role of synthesis conditions in controlling the resulting structure.

3.2.1 Sample Synthesis and Glass Structure

Figure 3.5 (a) and (b) display T_g of Samples at 31.6% homogenized at 1000°C for period t_h = 24 hours Such batch preparation shows fluctuations in T_gs of up to 20°C from one part of the sample to the other. These fluctuations come from spread in sample stoichiometry. Micro-Raman estimates of sample stoichiometry confirm the result. Figure 3.6 shows micro-Raman results of such a sample, and illustrate the intrinsic inhomogeneity.

Upon increasing t_h to 72 hours or more, fluctuations in T_g s decreased to 2°C as glass samples became homogeneous. These results are shown in the figure 3.7, figure 3.8. These T_g fluctuations examined at x = 31.6%, translate into compositional fluctuations in x of typically about 1.0 at.%, which is shown in figure 3.9.

3.2.2 Thermal Characterization

Glass transition temperatures were measured from the inflexion point of the reversing heat flow using a TA Instruments model 2920 T-modulated DSC. Figure 3.10

(a) displays MDSC trace of the stoichiometric glass at a scan rate of 3°C/min and a modulation rate of 1°C/100s and yields a T_g = 508°C. Here T_g is defined as the mean value of the inflexion point for scans up and then down in T. Defined as such, T_gs become not only independent of scan rate but also of sample thermal history. Figure 3.10 (b) gives a DSC trace of the same GeS_2 glass sample at a scan rate of 10°C/min and yields an apparent T_g (midpoint) of 502°C. Figure 3.11 provides a summary of the $T_g(x)$ trends with filled circles representing the MDSC results while the open triangles the DSC ones. Also projected in Fig. 3.11 is the DSC measured T_g (midpoint) = 491(5)°C of the GeS_2 sample used by Petri and Salmon [5], which may be compared to a value of 502°C for our GeS_2 sample measured under identical DSC scanning conditions. Petri and Salmon have performed elastic Neutron Scattering on their GeS_2 glass sample and inferred the pair correlation function from these studies. These results were used to model glass structure, an issue we discuss latter in chapter 4.

3.2.3 Raman Scattering

Figure 3.12 and Figure 3.13 (a) displays Raman lineshapes of GeS_2 and Ge-S glasses recorded at room temperature using a model T-64000 triple monochrometer system [6] from Instruments S.A., Inc. The back-scattered radiation was excited using 6mW of 514.5 nm in a conventional macro-Raman set up with glasses sample contained in the quartz tubes used for synthesis. The principal modes at 340 cm^{-1}, 360 cm^{-1}, and 440 cm^{-1} are assigned [2] to CS, ES and F_2 modes of $Ge(S_{1/2})_4$ tetrahedra. We have also
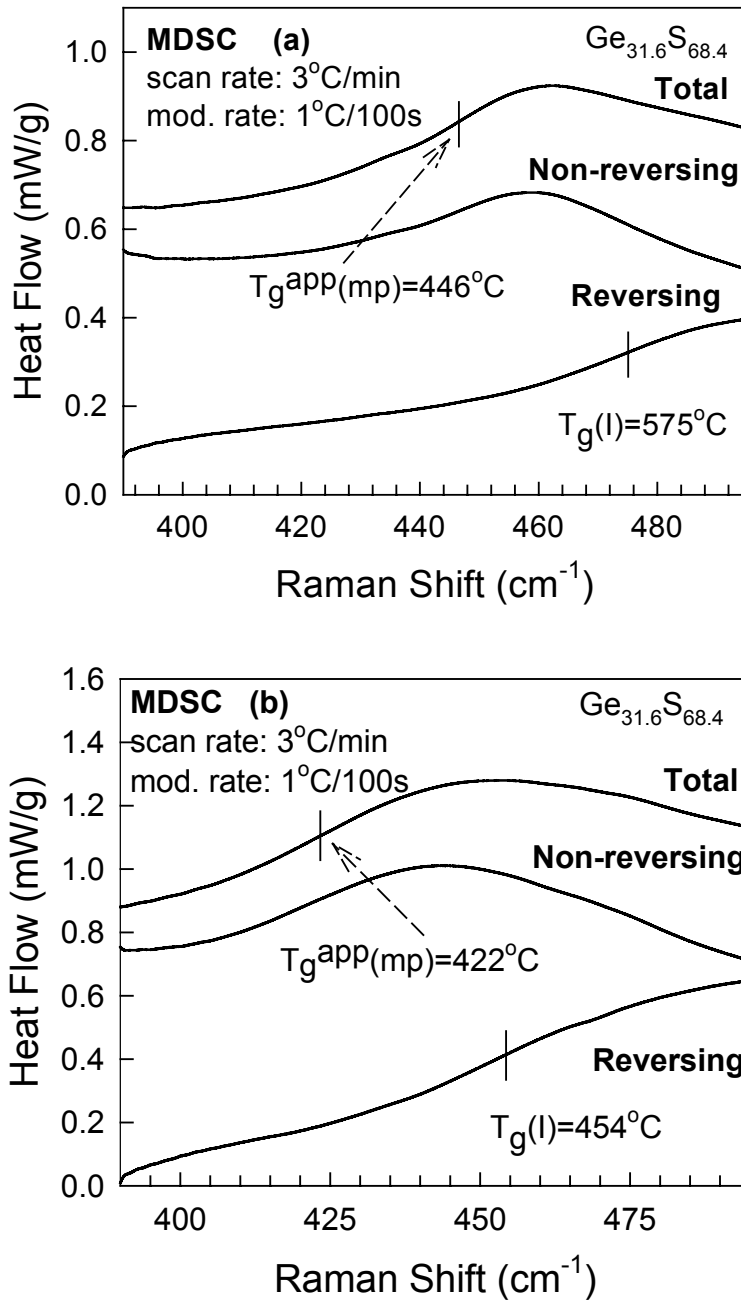
Figure 3.5 Glass transition temperature T_g of $Ge_{31.6}S_{68.4}$ glass samples from the same a batch preparation homogenized at 1000°C for t_h = 24 hours. (a) one part of sample. (b) another part of sample . Note fluctuations in T_gs of up to 24 °C from (a) and (b).
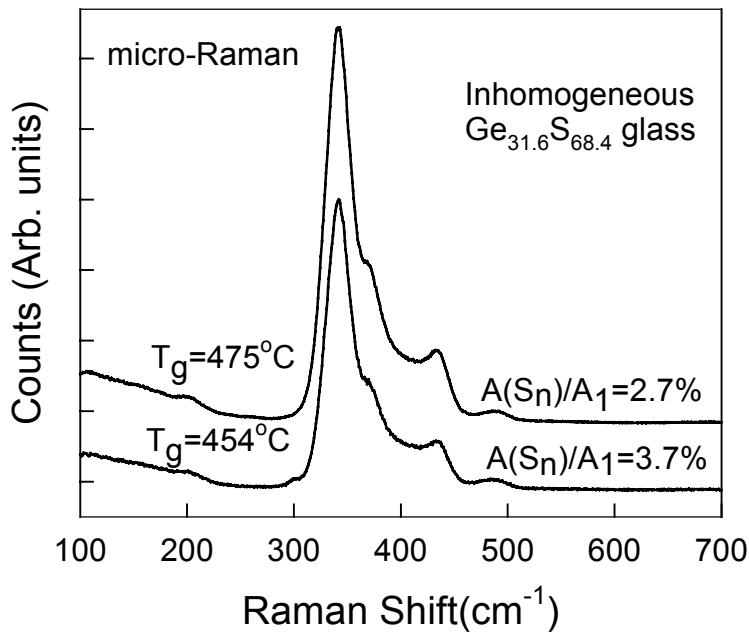
Figure 3.6 Micro-Raman scattering from $Ge_{31.6} S_{68.4}$ glass samples (a) and (b) of Figure 3.5 confirming spread in sample stoichiometry. The S-rich sample (b) has lower T_g as expected.
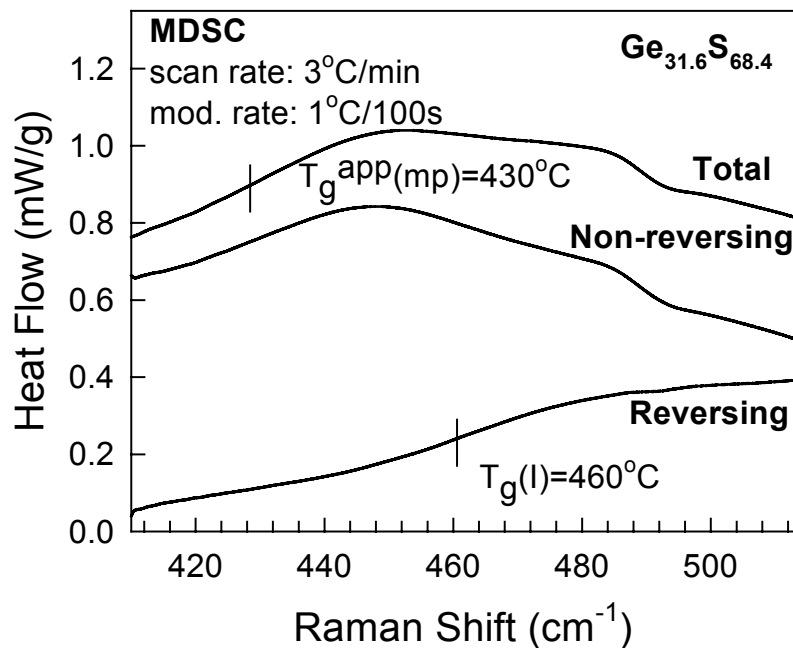
Figure 3.7 Glass transition temperature T_g of $Ge_{31.6} S_{68.4}$ glass homogenized at 1000°C for $t_h = 72$ hours showing a T_g of 460 °C, midway between those of samples (a) and (b) of Figure 3.5. This particular batch preparation shows a spread in T_g of less than 2 °C.
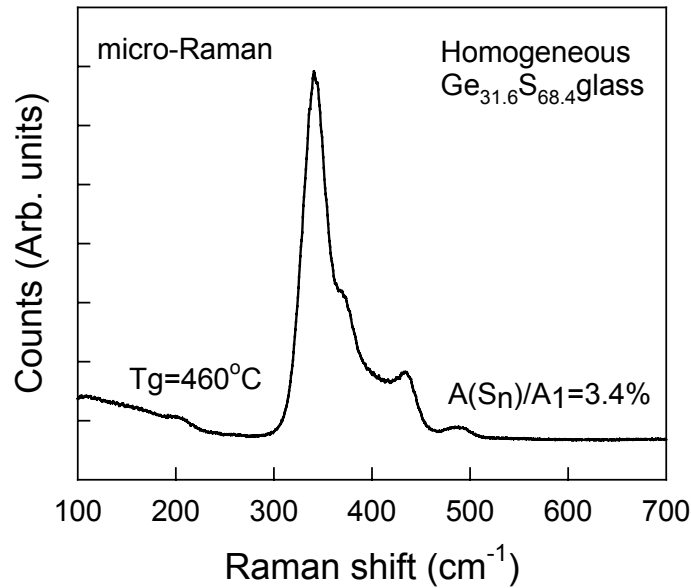
Figure 3.8 Micro-Raman scattering of $Ge_{31.6} S_{68.4}$ glass sample homogenized at 1000°C $t_h = 72$

hours. The sample is homogeneous.
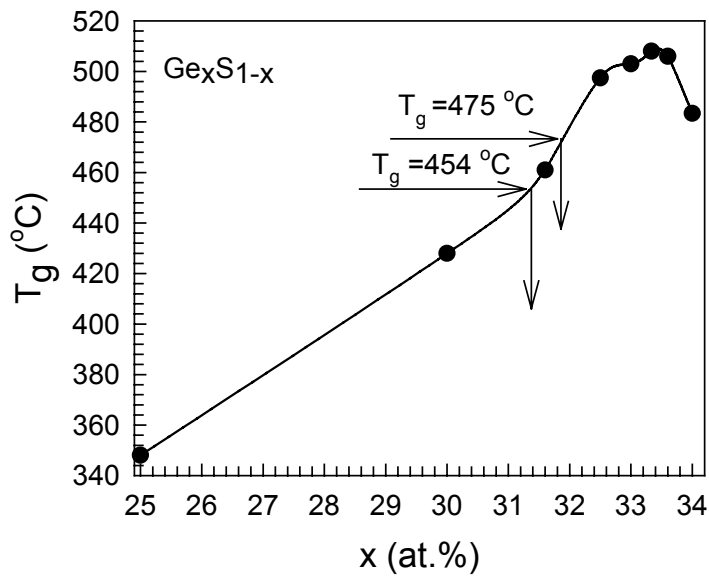
Figure 3.9 T_g (x) variation in homogeneous Ge_xS_{1-x} glasses. Fluctuations in T_g at x = 31.6%,

translate into compositional fluctuations in x of less than 1.0 at.%.
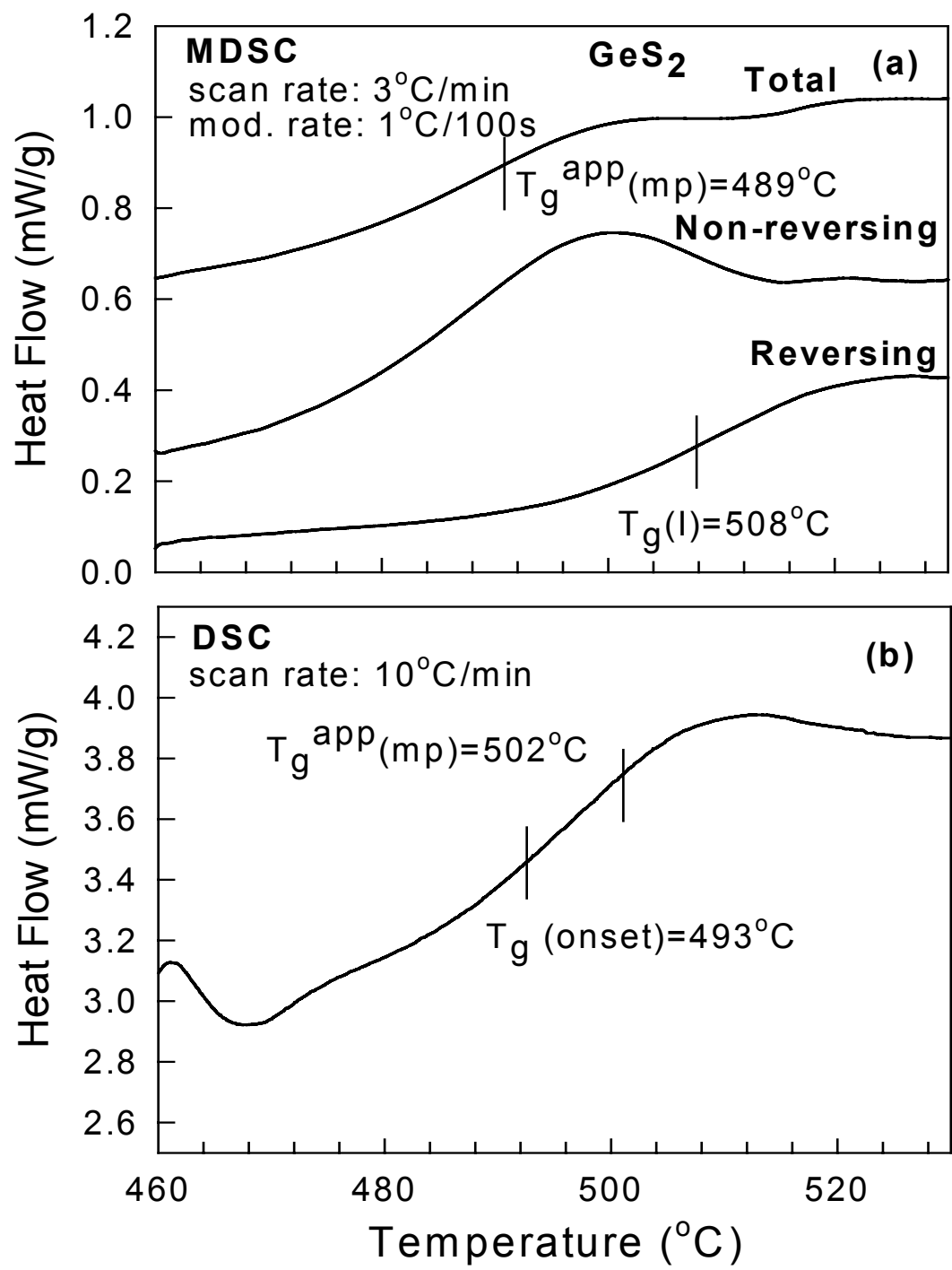
Figure 3.10 (a) MDSC scan of GeS$_2$ glass showing a T$_g$ of 508 °C, independent of scan rate. (b)

DSC scan of the same GeS$_2$ glass showing an apparent T$_g$ of 502 °C obtained at a scan rate of 10

°C/min.
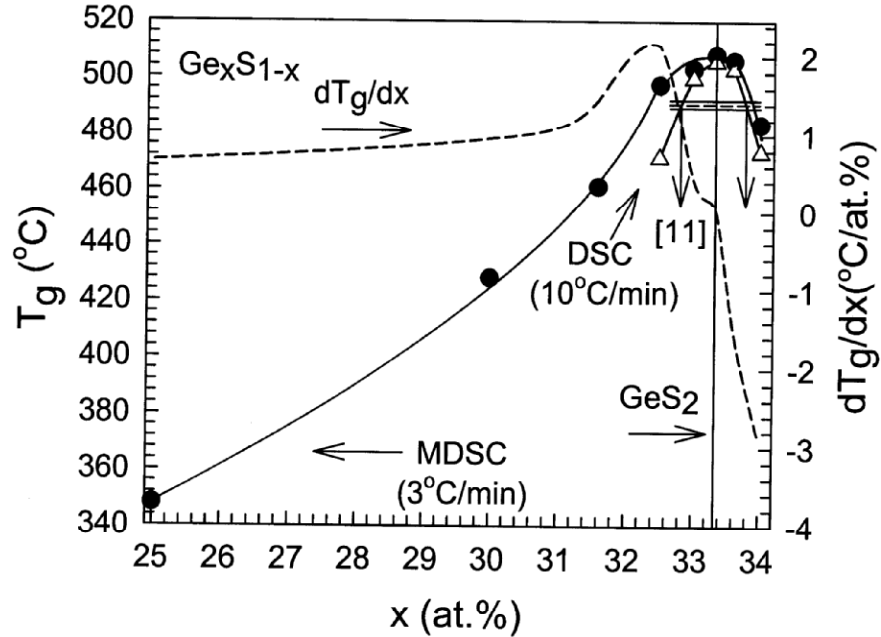
Figure 3.11 Compositional trend in T_gs of Ge_xS_{1-x} glasses obtained by MDSC (filled circles) and DSC scans (open triangles) showing a threshold behavior near x = 33.33. The horizontal strip projects the DSC measured apparent T_g of the GeS_2 glass sample used by Petri and Salmon in ref.4. The broken line curve gives the slope dT_g/dx of MDSC measured T_gs.

obtained the LO and TO IR response of our GeS_2 glass sample using a Nicolet model 870 FTIR, and the results appear as the broken-line curves in Figure 3.13 (b). The sharp features at 362 cm^{-1} and 449 cm^{-1} are ascribed to the strongly IR active F_2 modes of $Ge(S_{1/2})_4$ tetrahedra. Of special interest here are Raman modes observed in the 500 cm^{-1} and the 250 cm^{-1} regions that are enlarged in the right and left insets of Fig. 3.13 (a). One can discern the S_n-chain mode at 494 cm^{-1} in the right inset for samples at x = 32.5, 33.0 and 33.33, but not at 33.6 and 34.0. In the left inset one observes a pair of modes labeled

B at 255 cm^{-1} and labeled C at 236 cm^{-1}, that progressively grow in scattering strength

with increasing x starting at a threshold composition of x = 32.5.

Compositional trends in the scattering strength of the B and C modes normalized

to the A_1 mode (340 cm^{-1}) strength appear in Fig. 3.14 (a). At the stoichiometric

composition x = 33.33, the mode scattering strength ratio $A_B(255)/A_1$ = 0.036(5) and

$A_C(236)/A_1$ = 0.029(5). We assign the B-mode to ethane-like $Ge_2(S_{1/2})_6$ nanophase,

while the C-mode to distorted rocksalt $Ge(S_{1/6})_6$ nanophase as discussed later. The

presence of S_n-chain mode, B- and C-modes, shows that the stoichiometric glass is

chemically disordered.
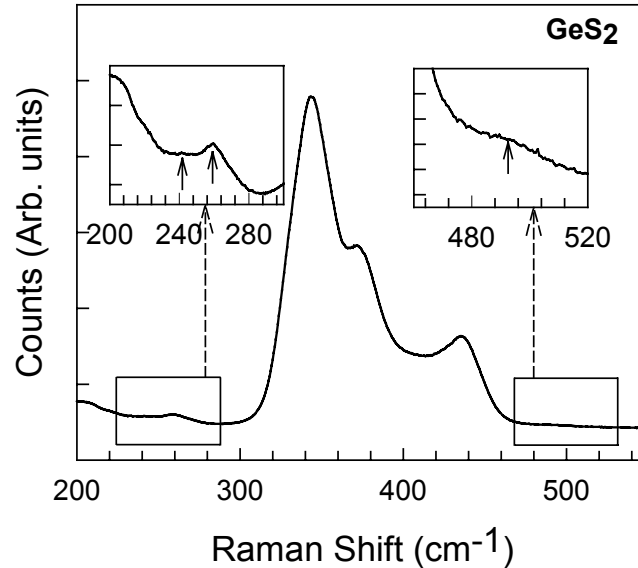
Figure 3.12 The Raman scattering of GeS_2 glass showing evidence of S-rich and Ge-rich

nanophases in the stoichiometric glass. The right inset shows a mode at 495cm^{-1} due to S-S

bonds. The left inset shows a pair of modes one at 240cm^{-1} ascribed to GeS and at 256cm^{-1} to

Ge_2S_6 unit. We discuss these issues in chapter 4.
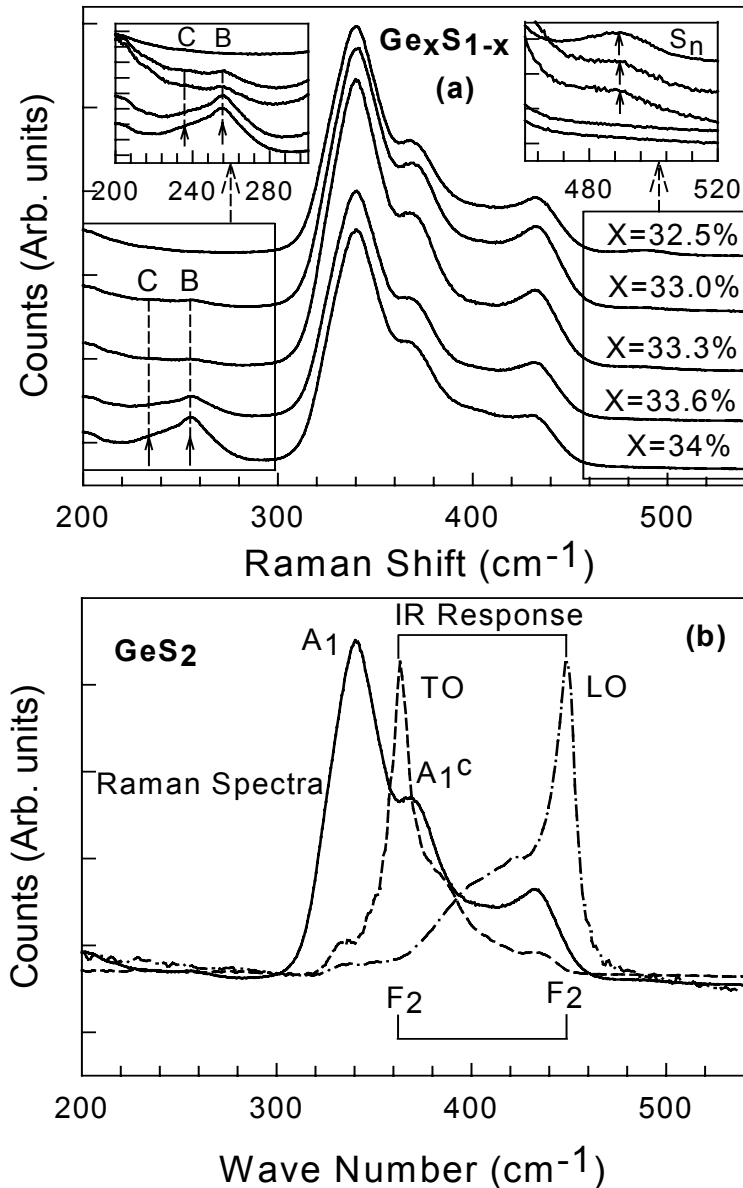
Figure 3.13 (a) Raman scattering in indicated glass samples obtained using 514.1 nm excitation in a macro-configuration. Note the presence of modes near 250 cm^{-1} and 500 cm^{-1} regions in the stoichiometric glass providing evidence of homopolar bonds. (b) Raman and IR response in GeS$_2$ glass showing contribution of A$_1$, A$_1^c$, and F$_2$ modes. to distorted rocksalt Ge(S$_{1/6}$)$_6$ nanophase as discussed later. The presence of S$_n$-chain mode, B- and C-modes, shows that the stoichiometric glass is chemically disordered.

3.2.4 ^{119}Sn Mössbauer Spectroscopy

$(Ge_{0.995}Sn_{0.005})_xS_{1-x}$ glasses doped with traces of enriched ^{119}Sn were independently synthesized and examined in ^{119}Sn Mössbauer spectroscopy measurements[3] at 78 K and at 4.2 K using an emitter of ^{119m}Sn in $CaSnO_3$. Figure 3.15.a displays the observed lineshape for a glass sample at x = 33.33 at 4.2K. The lineshape is dominated by a strong absorption centered near 1.6 mm/s and a weak satellite feature at 4.5 mm/s as also noted earlier [7]. Panels (b) and (c) show deconvolutions of the observed lineshape in terms of 3-doublets (A, B and C) and also 2-doublets [7] (A and B), respectively. The 3-site fit is a better fit and it also conforms to the Raman results. The all these ^{119}Sn Mössbauer spectra recorded at 78 K is displayed in figure 3.16. These figure from 3.17 to 3.21 are shown all separate ^{119}Sn Mössbauer spectra and their deconvoluitons of observed lineshape. Table 3.1 summarizes the quadruple splitting (Δ), isomershift (δ) and intensities (I). Figure 3.14 (b) provides a summary of the compositional variation of the integrated area, I_n/I under the A-, B- and C-doublets normalized to the total area. The B- and C-site integrated intensities systematically grow at the expense of the A-site one, once x > 32.5 at%. In particular at 4.2K, we obtain I_B/I = 0.17(2) and I_C/I = 0.15(1) for GeS_2 glass, reinforcing the conclusion from Raman scattering that the stoichiometric glass is chemically disordered.
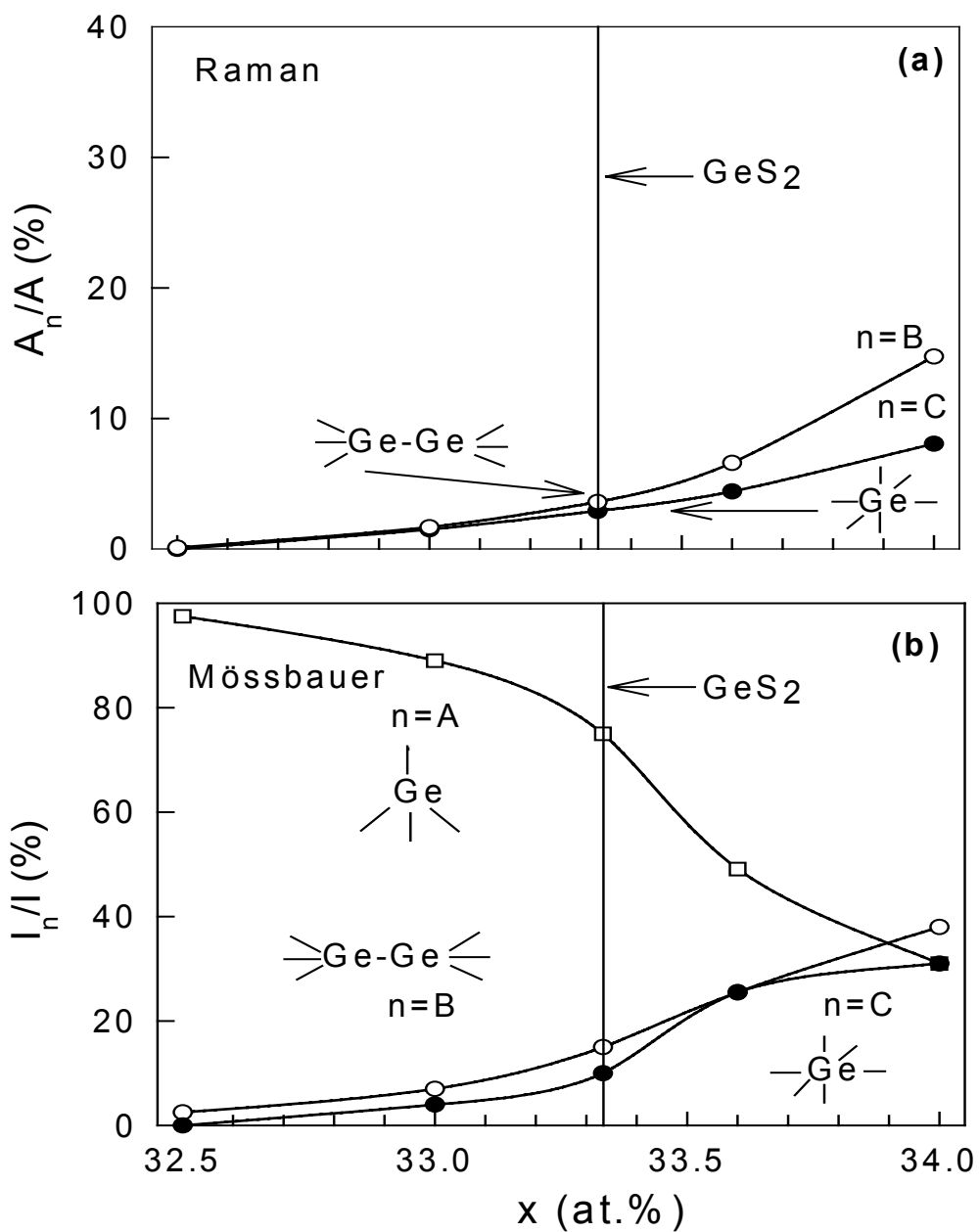
Figure 3.14 Compositional trends in (a) the normalized Raman scattering strengths of the B and C nanophase associated modes at 255 cm^{-1} and at 236 cm^{-1}. (b) The integrated intensity of the B-site and C-site doublets from [119]Sn Mössbauer spectroscopy.
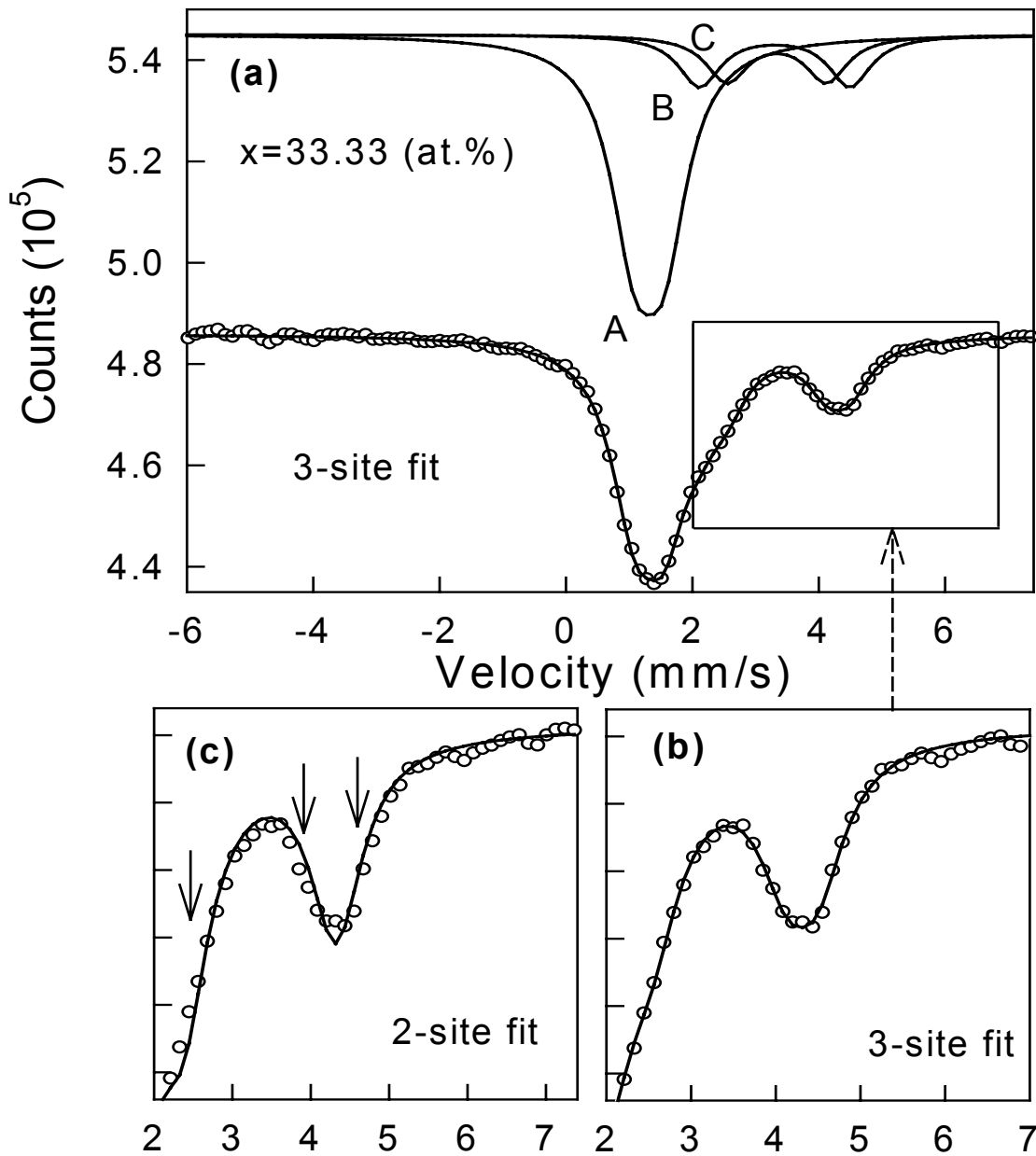
Figure 3.15 (a) [119]Sn Spectrum of a $Ge_{0.995}Sn_{0.005}S_2$ glass sample taken at 4.2 K. (b) and (c) panel show deconvolution of the line shape into 3 sites (A, B and C) and 2 sites (A, B), respectively. Systematic misfits appear at the arrows location when 2 sites are used.
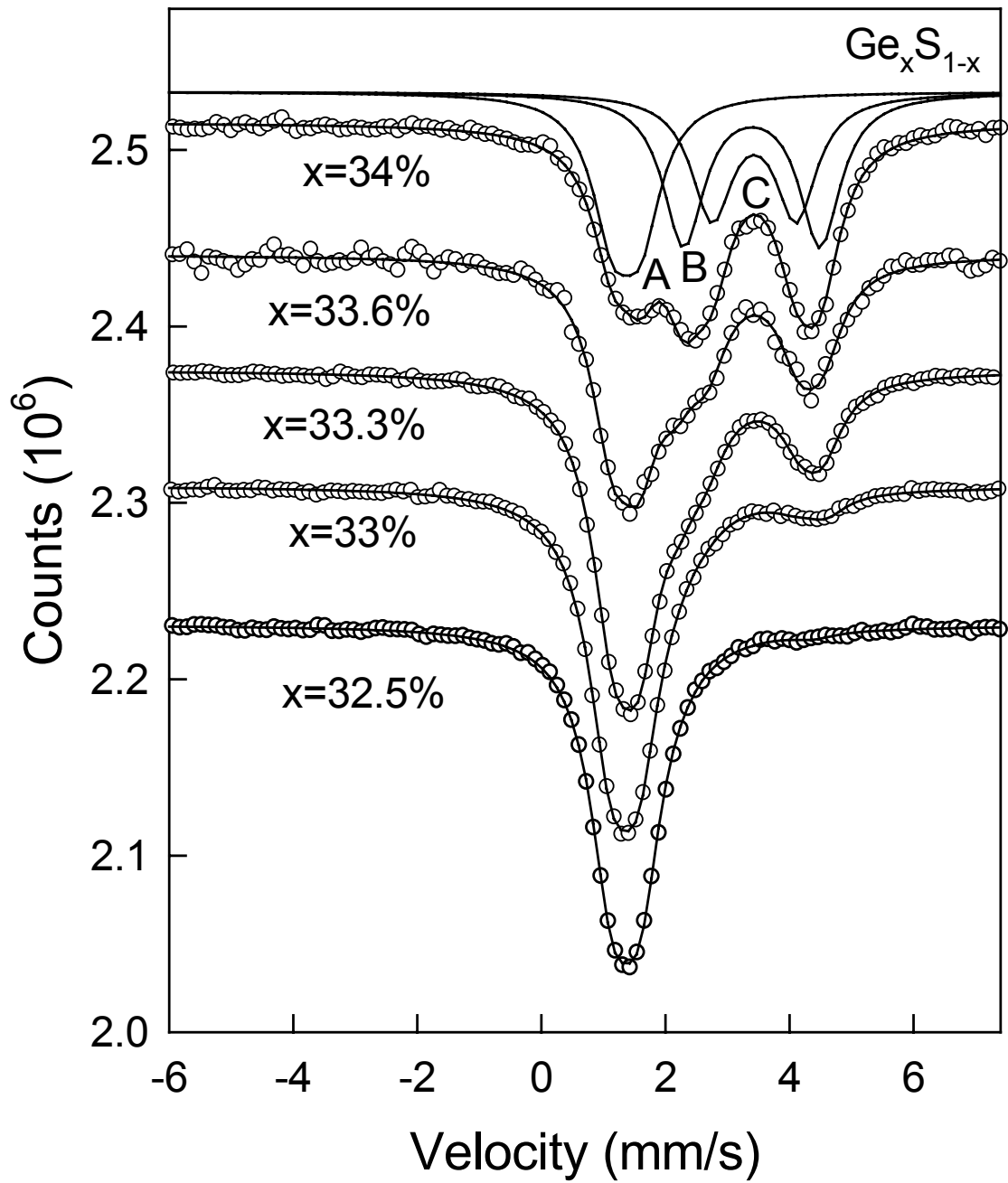
Figure 3.16 The all these [119]Sn Mössbauer spectra recorded at 78 K. The [119]Sn doped in all glass samples are half percent.
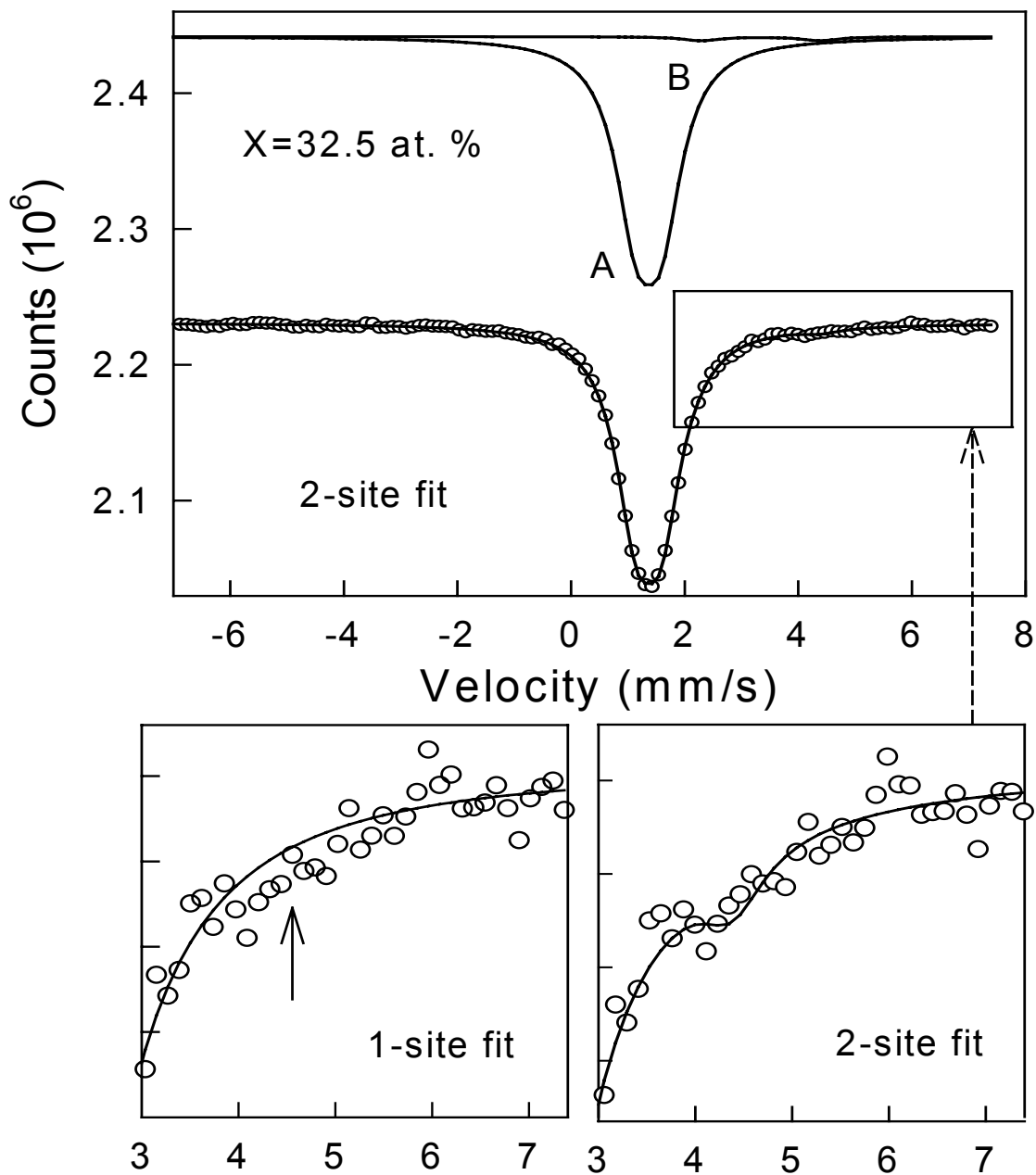
Figure 3.17 (a) [119]Sn Spectrum of a $(Ge_{0.995}Sn_{0.005})_{32.5}S_{67.5}$ glass sample taken at 77 K. (b) and (c) panel show deconvolution of the line shape into 2 sites (A,B) and 1 sites (A), respectively. Systematic misfits appear at the arrows location when 1 site is used.
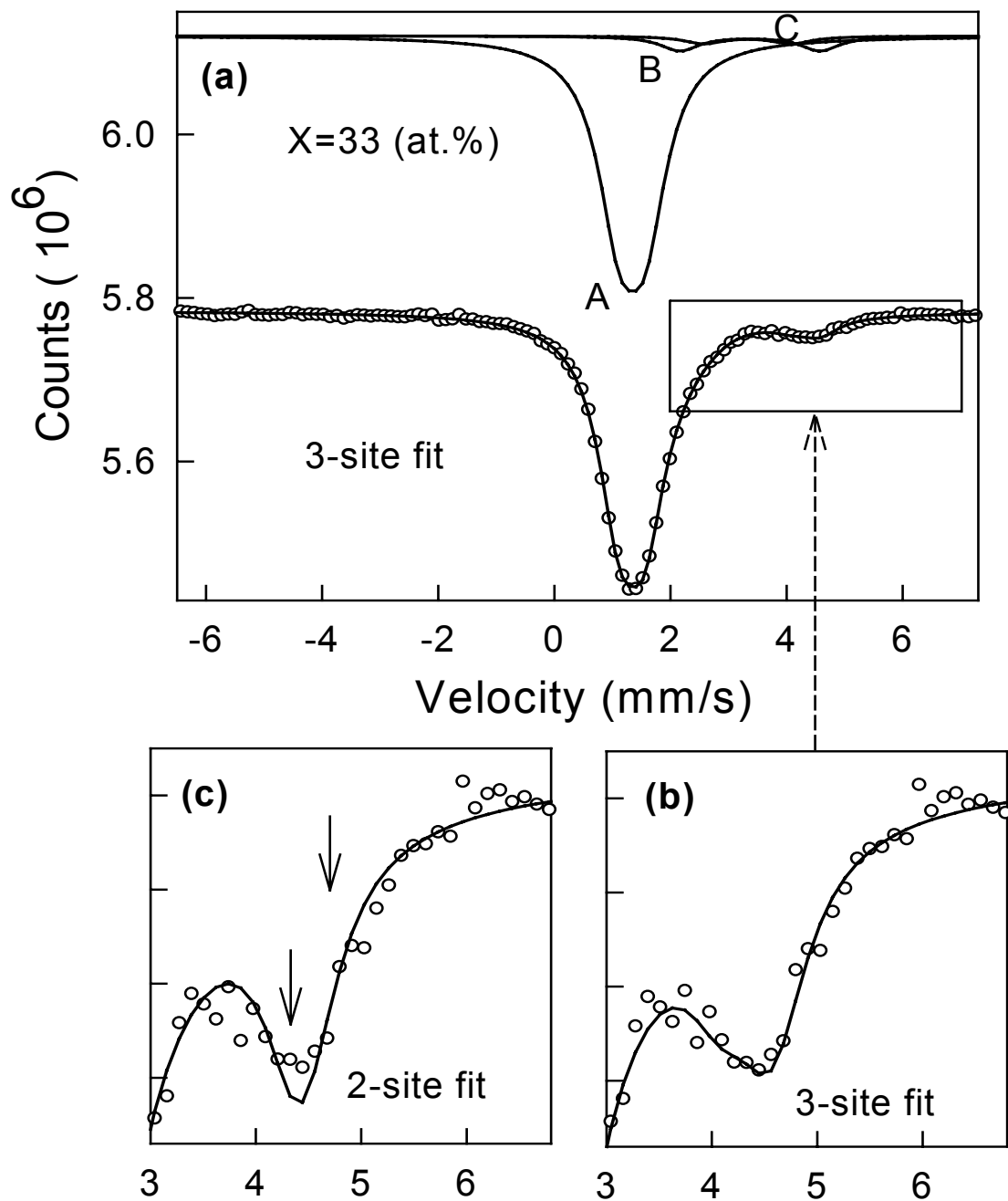
Figure 3.18 (a) ^{119}Sn Spectrum of a $(Ge_{0.995}Sn_{0.005})_{33}S_{67}$ glass sample taken at 4.2 K. (b) and (c) panel show deconvolution of the line shapes into 3 sites (A, B and C) and 2 sites (A, B), respectively. Systematic misfits appear at the arrows location when 2 sites are used.
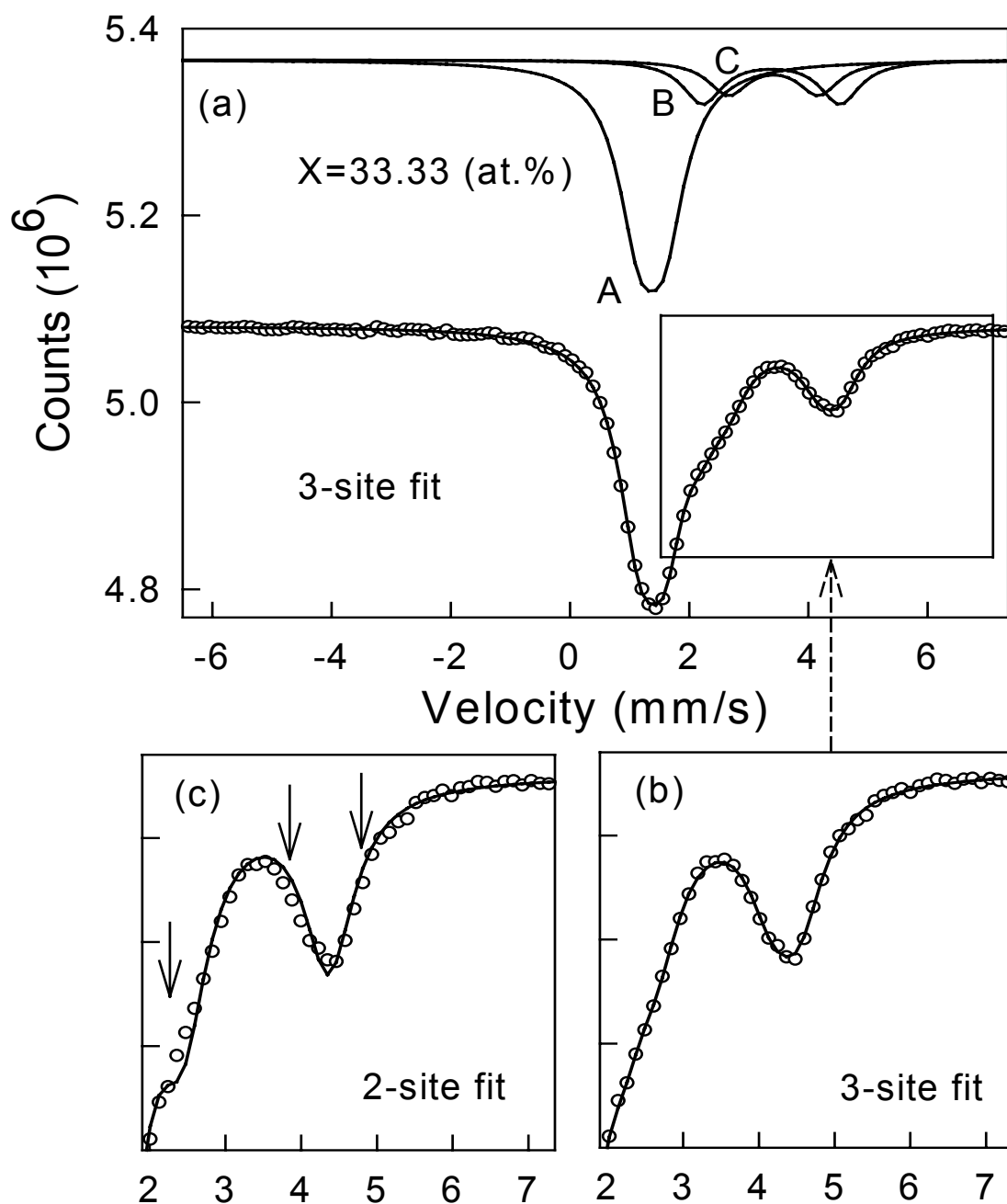
Figure 3.19 (a) ^{119}Sn Spectrum of a $Ge_{0.995}Sn_{0.005}S_2$ glass sample taken at 78 K.(b) and (c) panel show deconvolution of the line shapes into 3 sites (A,B and C) and 2 sites (A,B), respectively. Systematic misfits appear at the arrows location when 2 sites are used.
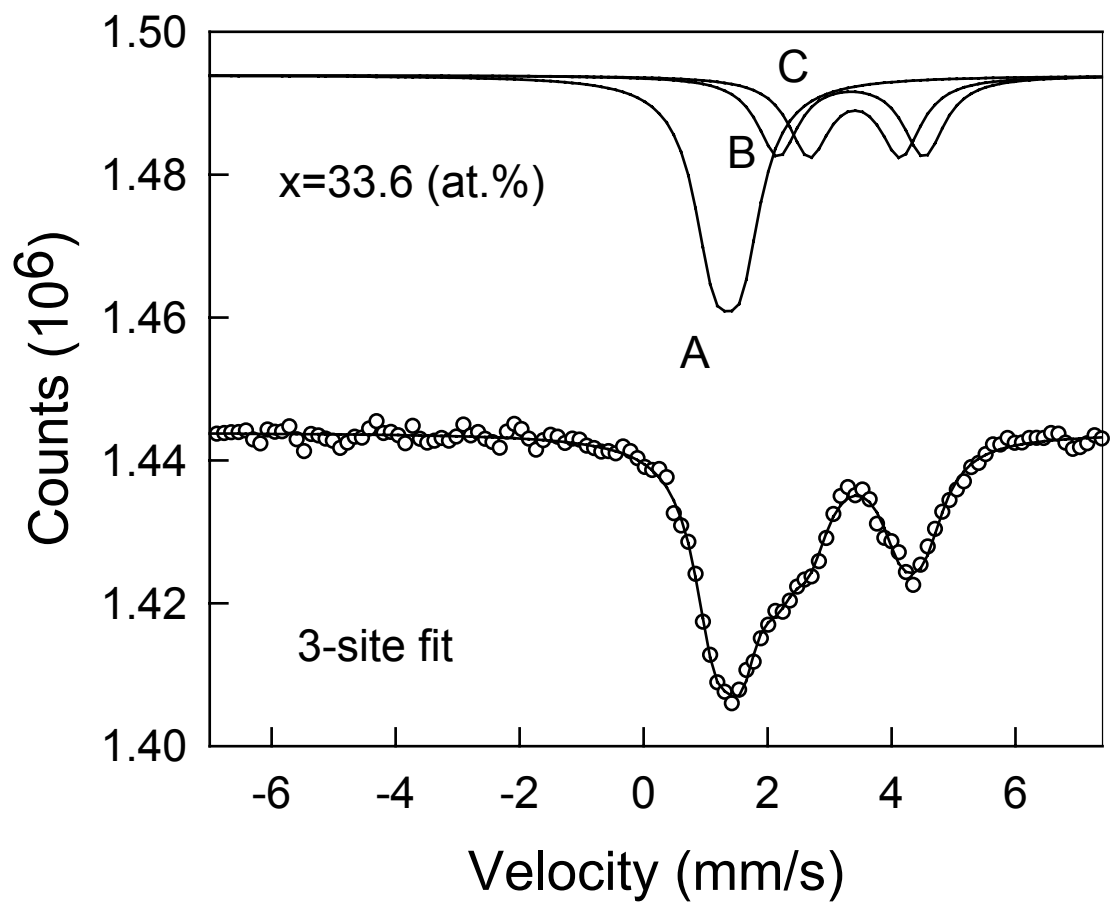
Figure 3.20 [119]Sn Spectrum of a $(Ge_{0.995}Sn_{0.005})_{33.6}S_{66.4}$ glass sample taken at 78 K. Deconvolution of the lineshqape into 3 sites (A,B and C) are shown.
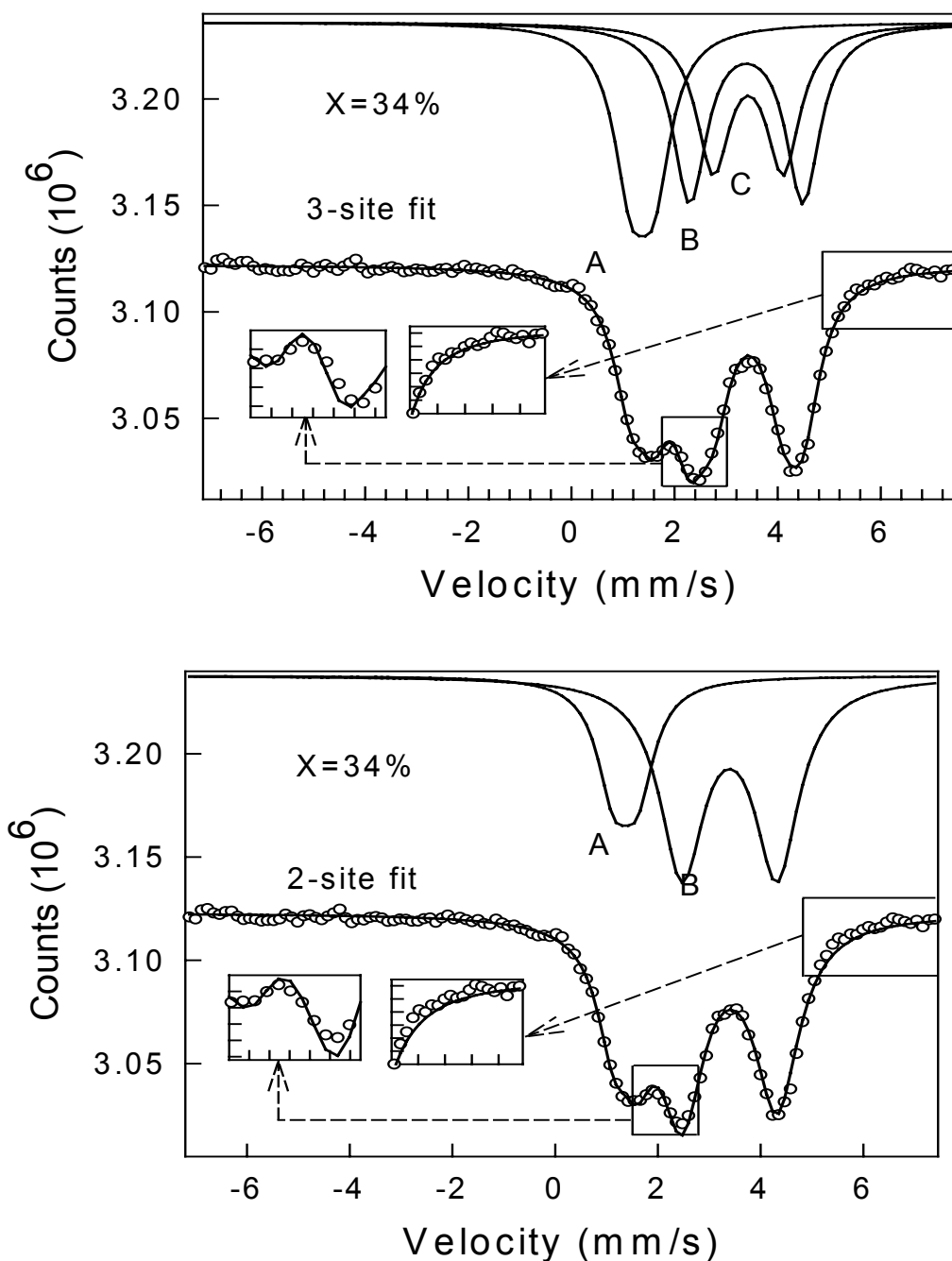
Figure 3.21 (a) ^{119}Sn Spectrum of a $(Ge_{0.995}Sn_{0.005})_{34}S_{66}$ glass sample taken at 78 K. (b) and (c) panel show deconvolution of the lineshqape into 3 sites (A, B and C) and 2 sites (A, B), respectively. Systematic misfits appear at the arrows location when 2 sites are used.

Table 3.1 Mössbauer isomershift (δ), quadrupole splitting (Δ) and integrated intensities of sites A, B and C observed in indicated $(Ge_{0.995}Sn_{0.005})_xS_{1-x}$ glasses at indicated temperature. The typical errors on δ and Δ parameters are $\pm$ 0.02mm/s.

x (at. %)	T (K)	Site Parameters (mm/s)						Site Intensities (A : B : C)
		A		B		C		
		δ	Δ	δ	Δ	δ	Δ	
32.5	78	1.33	0.45	3.26	2.18	—		97.5 : 2.5 : 0
33.0	78	1.33	0.45	3.35	2.42	3.32	1.52	89 : 7 : 4
33.33	78	1.32	0.43	3.30	2.28	3.33	1.56	75 : 15 : 10
33.33	4.2	1.32	0.47	3.30	2.27	3.33	1.57	68 : 17 : 15
33.6	78	1.32	0.44	3.31	2.36	3.37	1.48	49.0 : 25.5 : 25.5
34.0	78	1.33	0.45	3.35	2.20	3.34	1.36	31 : 38 : 31

3.3 Ternary $(GeS_2)_{1-x}(Ga_2S_3)_x$ Glasses

In section 3.2 we had presented results on GeS_2 glass. Here we present new results on pseudo binary $(GeS_2)_{1-x}(Ga_2S_3)_x$ glasses. These studies will permit us to understand the role of Ga_2S_3 additive in a base glass that is weakly nanoscale phase separated. We will present Raman Scattering and T_g results on these glasses. These results can be used to understand their molecular structure as will be discussed in chapter 4.

MDSC Results

Figure 3.22 display the glass transition temperatures as a function of x for $(GeS_2)_{1-x}(Ga_2S_3)_x$. These results were taken from MDSC measurements, in which the scanning rate and amplitude modulation rate were chosen as 3 ^{o}C/min and 1 ^{o}C/100sec,

respectively.   The figure shows us that T_g change with x. The Tg decreases with x increasing until x=17%. T_g reaches the minimum, which corresponds to the color of the samples shown in figure 3.23.

Raman Scattering

Figure 3.24 (a) and (b) and figure 3.25 display Raman Spectra taken at room temperature for $(Ga_2S_3)_x(GeS_2)_{1-x}$ glass. Figures 3.24 (a) and (b), 3.25 and 3.26 provide a summary of Raman scattering results on the titled glasses. At low x one observed growth in scattering strength of a band near 250cm^{-1}, and a progressive loss in strength of bands near 370cm^{-1} and 440cm^{-1} as x increases in the 0 <x < 15range. Furthermore the principal mode near 340cm^{-1} increases in that range.

At higher x, the observed lineshapes show the band near 250cm^{-1} to a new band near 260cm^{-1} to progressively increase in scattering strength with x in the 17 < x <35 range (figure 3.24 (b)). In these experiments, it was our experience that Raman scattering at x =17% was very weak. It was difficult to obtain a signed using red light (647nm) as the excitation source, probably because sample color turned dark brown (figure 3.23) as the optical gap of the glasses decreased below 2.0eV. But as x increased to 20% or higher, the Raman scattering signed increased qualitatively, we suppose because the sample color turned yellow or band gap increased to reach greater than 2.4 eV.

To better view changes in Raman lineshapes taking place near 250cm^{-1} we have blow up that segment of the scattering in figure 3.25. One can now see that bands B (256cm^{-1}) C (240cm^{-1}) growth with x at low x (0 < x <15%). At x > 20%, B- and C-bands sharply decrease in scattering strength and a new band appears near 262cm^{-1} labeled as C'.

The lineshapes were deconvoludted in terms of a superposition of Gaussian profiles. Variation in the normalized scattering strength of the A, B, C and C' bands are summarized in figure 3.26. One observes three district regimes as a function of (Ge$_2$S$_3$) content x of the glasses labeled I, II and III. Furthermore one can observe a clear correlation between these Raman scattering strengths and variation in T$_g$ (x) figure 3.22. These results can serve as a basis for a discussion of glass structure in section IV.
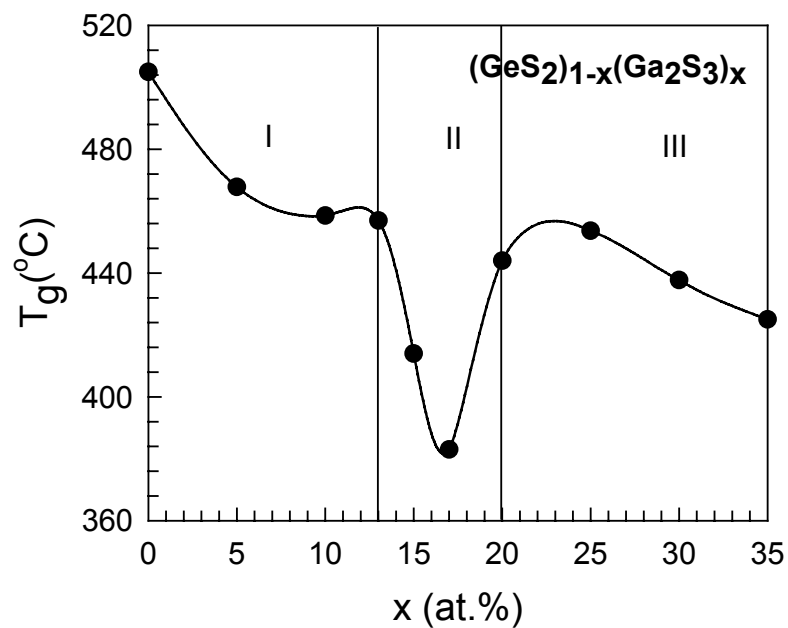
Figure 3.22 Glass Transition Temperature T_g of $(GeS_2)_{1-x}(Ga_2S_3)_x$ glasses for MDSC measurements showing a local minimum in region II near x=17%.
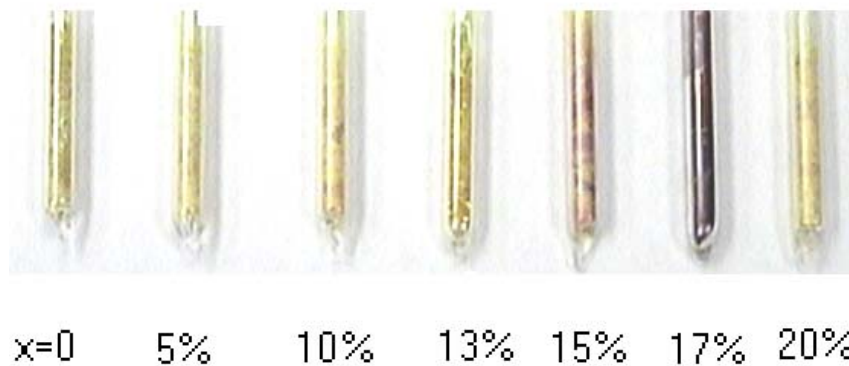
Figure 3.23 The color of $(GeS_2)_{1-x}(Ga_2S_3)_x$ samples showing a change with x. Samples at x=17% turned dark brown
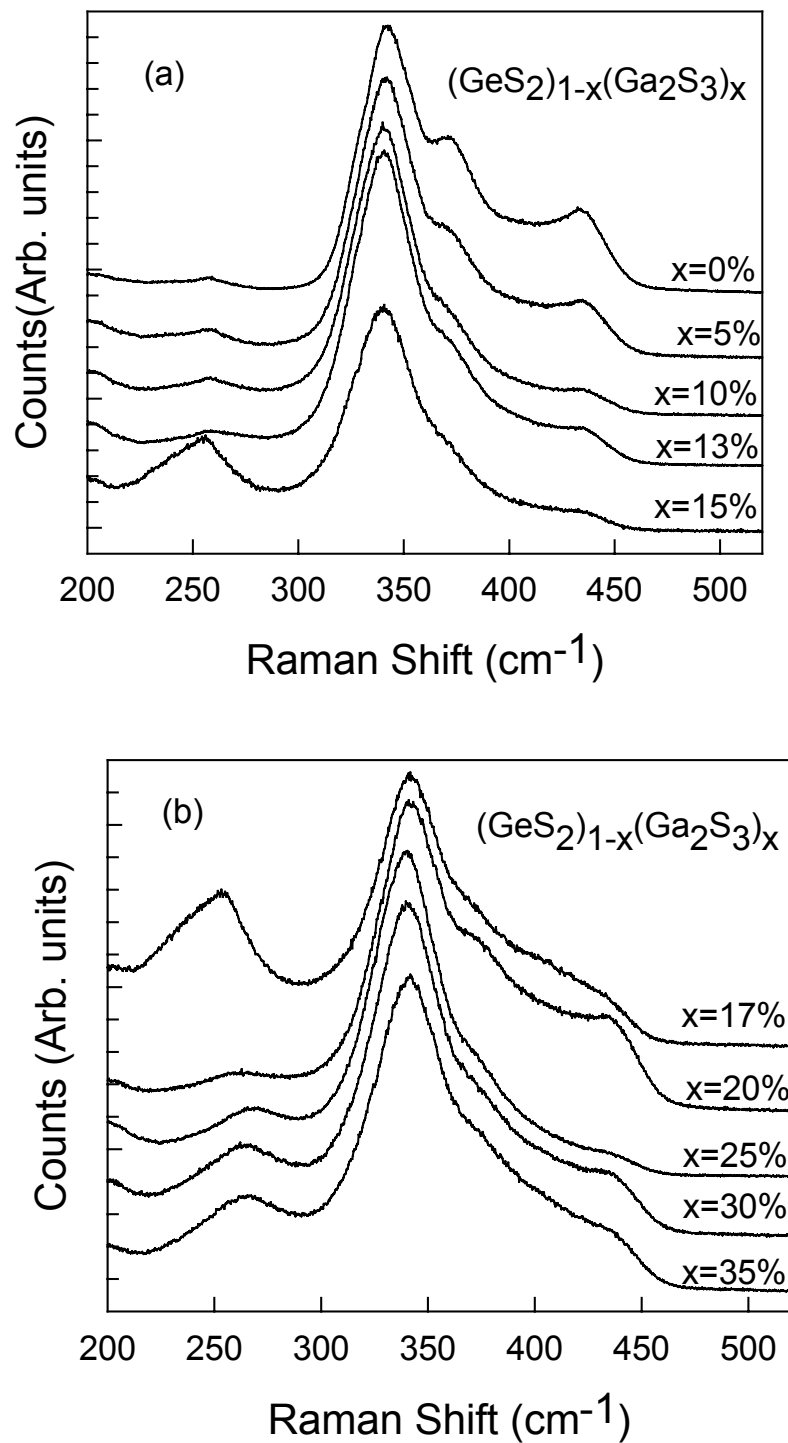
Figure 3.24 At (a) low x (0 < x <15%) and (b) high x (15% <x < 35%) showing evolution of 250cm^{-1} band near x =17%.
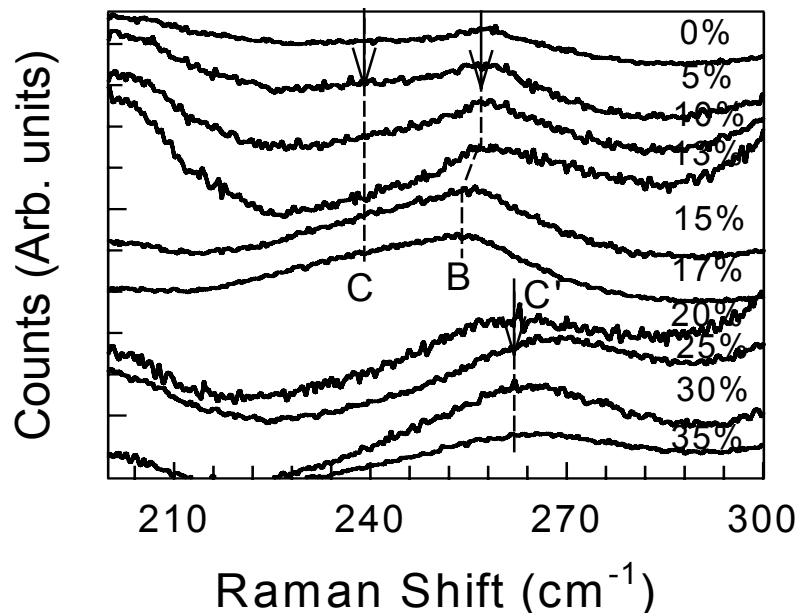
Figure 3.25 Details of Raman band evolution near 250cm^{-1} as a function of x in

$(GeS_2)_{1-x}(Ga_2S_3)_x$ glasses.
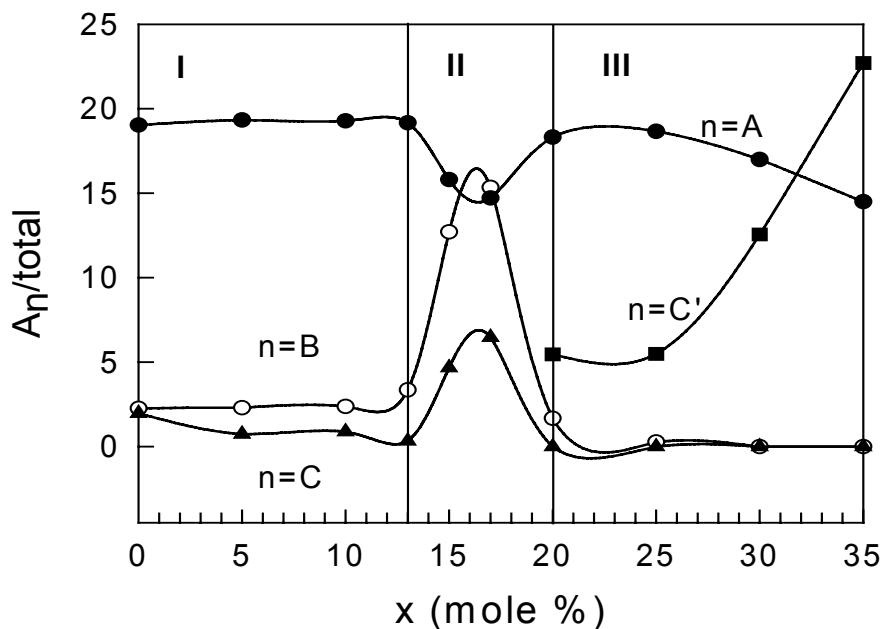
Figure 3.26 Variation in Raman scattering strengths of various bands n=A, B, C and C') I$_n$/I as a

function of x in $(GeS_2)_{1-x}(Ga_2S_3)_x$ glasses.

REFERENCES:

1. S. Mahadevan and A. Giridhar, J. Mon Cryst Solids **143** (1992), 52.

2. U. Tille, G. H. Frischat and K. J. Leers, Non-Crystalline Solids, (1977), 631.

3. R. Kerner and M. Micoulaut, J. Non Cryst Solids **210** (1997), 298.

4. A. Giridhar and Sudha Mahadevan, J. Non. Cryst Solids **151** (1992), 245.

5. I. Petri and P..S. Salmon, J. Non Cryst Solids **293** (2001), 169.

6. P. Boolchand, W.J. Bresser, Phil. Mag. B **80** (2000), 1757.

7. X. Feng, W.J. Bresser, P. Boolchand, Phys. Rev. Lett. **78** (1997), 4422.

8. P. Boolchand, J. Grothaus, M. Tenhover, M.A. Hazle and Robert K. Grasselli, Phys. Rev. B**33**, 5421 (1986). For a discussion of recoil-free-fraction considerations , see P.Boolchand, Vibrational Excitations in Glasses: Rigidity Transition and Lamb-Mossbauer Factors, *in Insulating and Semiconducting Glasses*, Ed. P.Boolchand, (World Scientific Press,Inc 2000)p. 369.

Chapter 4

DISCUSSION

In this section we propose to discuss three issues resulting from the results presented in Chapter 3: (a) Doping behavior of group III additive Indium in base Ge_xSe_{1-x} glasses; (b) the nature of molecular structure of the stoichiometric GeS_2 glass and (c) evolution of glass molecular structure in ternary $(Ga_2S_3)_x (GeS_2)_{1-x}$ glasses as a function of Ga_2S_3 additive.

4.1 Group III (Ga, In) Additive on Stressed Rigid Chalcogenide Glasses

New insights into the chemical alloying behavior of group III additives Indium in chalcogenide glasses have emerged from the compositional variation of glass transition temperatures. In this section we discuss the alloying behavior of Gallium and Indium in Ge_xSe_{1-x} glasses.

4.1.1 Indium Doping in Stressed Rigid (x>0.26) base Ge_xSe_{1-x} Glasses.

In a series of rather impressive set of measurements of T_g and molar volumes in the ternary Ge-In-Se system, S. Mahadevan and A.Giridhar [1] found that the threshold behavior of $T_g (\bar{r})$ near $\bar{r} = 2.67$ observed at $y = 0$, i.e., binary Ge_xSe_{1-x} glasses, shifts rather systematically (figure 4.1) to lower values of r as In content (y) of ternary

$Ge_xIn_ySe_{1-x-y}$ glasses increases in the $0 < y < 0.15$ range. The existence of the threshold shift to low $\bar{r}$ suggests that nanoscale phase separation must occur. For trivalent In species, one can generally write,

$$Ge_xIn_ySe_{1-x-y} = (5y/2)(In_{2/5}Se_{3/5}) + Ge_xSe_{1-x-5y/2} \tag{1}$$

In the present case, the first and second terms on the right hand side of equation 1 describe respectively, the In-rich nanophase, and the left over base glass phase. Because of such separation, the base glass can nanaoscale phase separate [2] when the Ge/Se stochiometry ratio exceeds the threshold value of ½ corresponding to a chemical threshold, i.e.,

$$x / (1-x-5y/2) = ½ \tag{2}$$

Thus, for a given In content (y), equation 2 serves to define a critical mean coordination number,

$$\bar{r_c} = 2 + 2x_c + y = (8-2y)/3 \tag{3}$$

when the ternary glass is expected to display a local maximum in T_g. In Figure 4.3, the straight line represents a plot of equation 3, while the data points are the observed thresholds reported [1] by S.Mahadevan and A. Giridhar. The correlation between theory and experiments is excellent. The central message is that in the present ternary the additive segregates into an In-rich nanophase (equation 1) soaking Se from the base glass, and thereby driving the base glass to become Ge-rich and eventually phase separate into a Ge-rich and a Se-rich nanophases.

A very similar physical picture of alloying Ga in Ge-Se glasses emerges from T_g trends in figure 4.2 and in figure 4.3 .The threshold behavior of T_gs so characteristic of

the base glass (Ge-Se) near $\bar{r}$ = 2.67, is also observed upon Ga alloying. The results of Figure 4.2 are also based on the work of S.Mahadevan and A. Giridhar [1]. The figure 4.1 is taken from ref. [3].

These results demonstrate that the group III additives "Ga" and "In", chemically bond with Se to form Ga_2Se_3 or In_2Se_3 clusters to leave behind a Ge-rich base glass as Se is removed from it. The base glass eventually nanoscale phase separates when the additive concentration reaches a threshold. The latter occurs when the Ge : Se ratio approaches to 1 : 2. The plot of figure 4.3 shows variations in $x_c(y)$ prescribed by such a model. The data points correspond to the results of S. Mahadevan and A.Giridhar. The excellent fit between theory and experiment serves to demonstrate that in stressed rigid glasses, i.e. x > 0.25 the group III additives do not form part of the backbone. They segregate into Ga- or In- rich clusters.
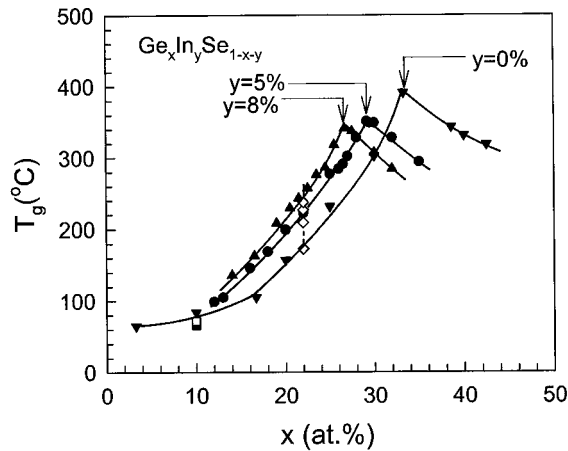
Figure 4.1 T_g (x) variation in ternary $Ge_xIn_ySe_{1-x-y}$ glasses taken from ref. [3], showing a threshold behavior at a fixed In concentration y. The threshold x_c systematically moves to lower values as the In concentration (y) increases. Present MDSC T_g in Ge22InySe78-y glasses are shown as open squares (◊), and are in harmony with those reported in [3].

60
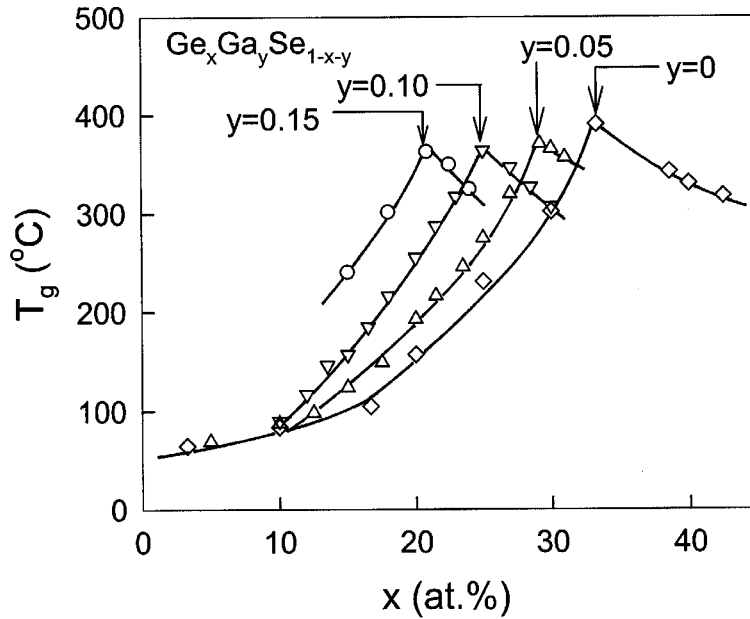
Figure 4.2 Variations in T_g (x) of ternary $Ge_xGa_ySe_{1-x-y}$ glasses showing a threshold behavior near $x=x_c$ at indicated Ga concentration y. The threshold x_c systematically shifts to lower values of x as the Ga concentration (y) increases. The figure is taken from ref.[1]. T_gs are measured using DSC.
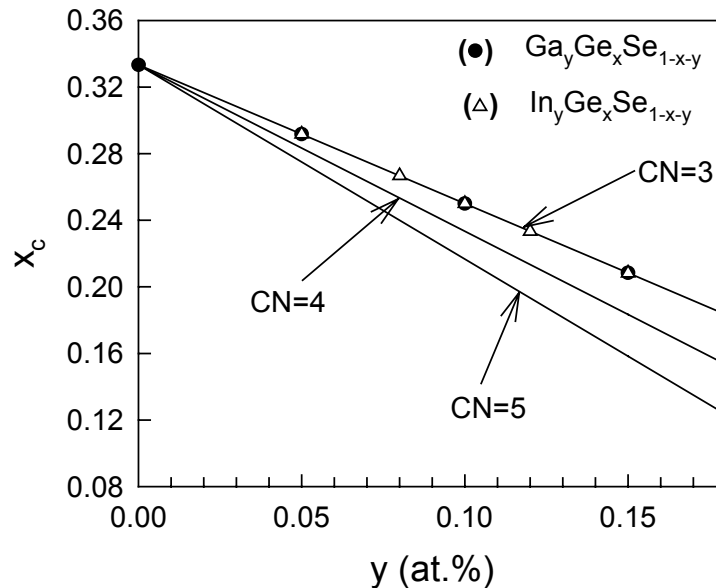
Figure 4.3 The predicted variation in the threshold concentration of Ge, x_c, where T_g (x) values show a maximum against Ga or In concentration [4].

61

4.1.2 Indium Doping in Self-Organized (x=0.22) Base Ge_xSe_{1-x} Glasses

In the intermediate phase of Ge_xSe_{1-x} glasses, such as a composition $Ge_{22}Se_{78}$ glass for example, alloying group III additives also leads to an increase of T_g. Variations in the glass transition temperature, $T_g(x,y)$, in $Ge_{22}In_ySe_{78-y}$ glasses reveal a slope dT_g/dy near x=0.22 of 8.2, that may be compared to the base glass slope, dT_g/dx in Ge_xSe_{1-x} glasses near x=0.22, of 10.8 as shown in figure 3.2. The base glass slope was obtained form figure 2 taken from ref. 2. These slopes dT_g/dy and dT_g/dx are quite close to each other although they are not exactly the same. If these were identically the same, a possible interpretation of these slopes would be that In-doping behavior is just like Ge doping. This is to say that Indium like Ge enters the base glass *tetrahedrally coordinated*. But there is another attractive possibility of the interpretation of the slope dT_g/dy =8.2 $^oC/at/\%$ In in $Ge_{22}In_ySe_{78-y}$ glasses. As in stressed rigid glasses, In could combine with Se to form In_2Se_3 nanocrystalline phase, and segregate from the base glass. If this is the case, then the following equations will describe the underlying NSPS.

$$Ge_{0.22}In_y\,Se_{0.78-y} = 2.5(In_{0.4}Se_{0.6}) + Ge_tSe_{1-t} \qquad\qquad (4)$$
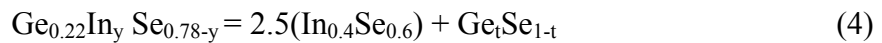
$$\text{with} \qquad t = 0.22/(1-2.5y) \qquad\qquad (5)$$

One would expect $T_g(y)$ to increase as a function of y largely because the remaining base glass (Ge_tSe_{1-t}) would become progressively Ge-rich (t > 0.22) as the In additive concentration 'y' is increased in the alloyed glasses. One can estimate the

increase in $T_g(y)$ anticipated by calculating t for a given value of y, and then obtain T_g for the base glass form the observed $T_g(x)$ in Ge_xSe_{1-x} glasses (ref.2).

Table 4.1 Variations in T_g with y based on above cluster model in $Ge_{0.22}In_y Se_{0.78-y}$ glasses.

y	t	$T_g{}^{pred}$
0	0.22	209.4
0.02	0.232	226.2
0.05	0.252	251.3

$$(dT_g/dy)_{y\to0}{}^{pred} = 8.4$$

As shown above in table 4.1 the variation in T_g with y based on such a cluster model, permits us to calculate an average value of dT_g/dy at low y of 8.4 ^oC/at/% In. The predicted slope $(dT_g/dy)^{pred}$ compares very well with the observed slope $(dT_g/dy)_{exp} = 8.2$ (figure 3.2). The agreement shows persuasively that our model of NSPS of In additive in $Ge_{22}Se_{78}$ glass is very plausible.

Finally, the results of figure 3.2 also serve to demonstrate that there is limited solubility of "In" in $Ge_{22}Se_{78}$ glass of less to 8%. At higher In concentrations, T_g and ΔH_{nr} drop remarkably. And it appears above 3% of In continues to be in the base glass as In_2Se_3 with the rest segregating as In clusters. This is one possible interpretation of the sharp reduction of T_g and ΔH_{nr} once y = 10% in figure 3.2. XRD measurements would help clarify the interpretation.

Our final comment pertains to group V (Sb, As) additives in $Ge_{20}Se_{80}$ base glass. The observed DSC slopes with Sb or As additives in $Ge_{20}Se_{80}$ glasses are found to be 7.1 and 6.8. It is generally believed that these group V additives enter these base glasses as 3-fold coordinated to Se neighbors in a pyramidal local structure. The base glass slope dT_g/dx of Ge_xSe_{1-x} glasses near x=0.20 in DSC measurements is found to be 14.75. The exact implications of these results are still not clear.

4.1.3 *Indium Doping in Floppy (x=0.10) base Ge_xSe_{1-x} Glasses*

The present MDSC results on "In" doping in $Ge_{10}Se_{90}$ base glass yield a slope of $dT_g/dy=2.2$ ^{o}C/at% In. It is smaller than the MDSC base glass slope of 4.6 ^{o}C/at% Ge. It is useful to consider a model in which "In" does not enter the base glass either as 3-fold or as 4-fold but segregates as In_2Se_3 clusters.

In the extreme floppy limit of a Se glass, there are EXAFS reports to suggest that In segregates from the base glass into In_2Se_3 microcrystalline clusters. In this dilute limit of a Se glass, $dT_g/dy \rightarrow 0$, understandably because segregation of In_2Se_3 clusters does not change the stoichiometry of the base glass. On the other hand, in a $Ge_{10}Se_{90}$ base glass, as In_2Se_3 clusters decouple from the base glass, one expects the latter to become progressively Ge-richer, and T_gs to increase .We can calculate the expected increase of T_g within such a phase-separated model as follows:

$$Ge_{0.1}In_ySe_{0.9} = 2.5y(In_{0.4}Se_{0.6}) + Ge_tSe_{1-t} \tag{6}$$

On balancing the stoichiometry, we find,

$$t = 0.1/(1-2.5y) \tag{7}$$

Table 4.2 Variations in T_g with y based on above cluster model in $Ge_{0.10}In_ySe_{0.90-y}$ glasses.

y	t	T_g^{pred}
0	0.10	105
0.1	0.133	125
0.133	0.15	133

$$(dT_g/dy)_{y\to0}^{pred} = 2.1$$

Relation (7) suggests that as In is alloyed in the base glass, the base glass becomes Ge-rich, as In_2Se_3 clusters form. In particular, $t = 0.10$ at $y = 0$, but $t = 0.133$ at $y = 0.10$. The base glass T_g at $t = 0.10$ and $t = 0.15$ is 105^oC and $133 ^oC$, yield a slope of 2.1 ^oC/at% Ge. The result is in reasonable agreement with the observed slope of 2.2 ^oC/at% In, which is shown in table 4.2.

In summary, it appears that the oversized group III additive indium segregates into In_2Se_3 clusters in a $Ge_{10}In_y Se_{90-y}$ glasses. This behavior has also been noted by Saiter [20-21] et al. for elemental glass Se and binary Ge-Se glasses from EXAFS [20-21] measurements. Finally, it is appropriate to comment on DSC based T_g variations with Sb or As additives in Ge_xSe_{1-x} base glass as reported in literature [22-23]. Here, the slope,

dT_g/dy, observed in (As or Sb)$_y$Ge$_{10}$Se$_{90-y}$ glasses, are found to be 3.52^{o}C/at% As and 3.4 ^{o}C/at% Sb. The base glass (DSC) slope dT_g/dx near x=0.1 is found to be 3.0. In the stochastic limit these slopes can be calculated using SAT. In general, one expects the base glass slope dT_g/dx, where Ge is 4-fold coordinated to be lower than the slopes with group V additives which all thought to be 3-fold. These calculations have not been performed yet but we anticipate working with M. Micoulaut to examine the issue further.

In summary, MDSC results on In doped Ge$_x$Se$_{1-x}$ glasses over all ranges x, i.e. floppy (0 < x < 0.20) , intermediate (0.20 < x < 0.26) and stressed rigid (0.26 < x < 1/3) reveal that the group III additives nanoscale phase separates as In$_2$Se$_3$ phase leaving behind a Ge-rich base glass. The observed slopes, dT_g/dy, in Ge$_x$In$_y$Se$_{1-y}$ glasses can be are in excellent accord with the predicted slopes based on a   nanoscale phase separated model in which In is trivalent and is bonded to 3/2 Se atoms shown in table 4.3. The covalent radius of In (1.405Å) exceeds that of Ge(1.225 Å) [5] by 15%. These results demonstrate that large size mismatch between atoms can drive nanoscale phase

Table 4.3 The observed slopes, dT_g/dy, in Ge$_x$In$_y$Se$_{1-y}$ glasses. The predicted slopes based on a nanoscale phase separated model and the slopes, dT_g/dx in base Ge$_x$Se$_{1-x}$ glasses are compared in table.

Phases	$(dT_g/dy)_{obsv.}$	$(dT_g/dy)_{pred.}$	$(dT_g/dx)_{base}$
Floppy	2.2	2.1	4.6
Intermediate	8.2	8.4	10.8
Stress Rigid	$x_c(y)$ predictions fit observations perfectly as described in Fig. 4.3		

separation in network glasses. These results were obtained using a thermal method that is *not* generally recognized as a structural probe of network glasses. In that respect these results are not only new but quite novel.

4.2 Nano-Phase Separation of GeS$_2$ Glasses

GeS$_2$ glass in analogy to the high-T crystalline phase (α-) of GeS$_2$ is widely believed to consist of a chemically ordered fully polymerized network of CS- and ES-Ge(S$_{1/2}$)$_4$ tetrahedral units[24]. This view comes largely from analysis of neutron structure factors by first principles molecular dynamic simulations. At some level of sophistication, the average global structure, this picture of the s stoichiometric glass is acceptable. Profound details of glass structure are now available from local probes like Raman scattering, Mössbauer spectroscopy and MDSC, as examined by us in this work. These latter probes reveal that a finite concentration of non-tetrahedral Ge sites occur in the stoichiometric glass showing the glass, unlike the crystal, is not chemically ordered. Furthermore, trends in T$_g$(x) in Ge$_x$S$_{1-x}$ glasses show that these non-tetrahedral local structures do not form part of the tetrahedrally coordinated base glass network. The non-tetrahedrel local structures form separate nanaphases, lowering the global connectedness of the backbone that is reflected in the rate at which T$_g$(x) varies near x=1/3. These ideas lead to nanoscale phase separation of the base glass, as we show here. Both the Raman scattering and [119]Sn Mössbauer spectroscopy by provide evidence for non-tetrahedral Ge in stoichiometric GeS$_2$ glass as described in chapter. Details on interpretation of these site and vibrational signatures are given below.

4.2.1 Origin of Broken Chemical Order in GeS$_2$

Both the Raman scattering and ^{119}Sn Mössbauer spectroscopy provide evidence for non-tetrahedral Ge in stoichiometric GeS$_2$ glass as described in chapter 3. Interpretation of these site and vibrational signatures are discussed below.

A first principles density functional calculation of vibrational modes on selective GeS$_n$ clusters has shown [6] that ethane-like Ge$_2$ (S$_{1/2}$)$_6$ units possess two strongly active Raman modes; one at 254 cm^{-1} and the other at 366 cm^{-1}. These calculations [6] provide justification to assign the mode at 255 cm^{-1} to the presence of ethanelike units [7]. Our Raman spectra also reveal a mode at 236 cm^{-1}, and it is assigned to the presence of distorted rocksalt Ge(S$_{1/6}$)$_6$ units in analogy to the A$_g$ mode observed [4.,8] in c-GeS at 238 cm^{-1}. The cluster calculations [6] also show the Raman cross-section of the 254 cm^{-1} mode to be nearly half that of the 340 cm^{-1} mode, suggesting that the concentration of ethanelike units to CS tetrahedral units is 7.2%. Since there are 2 Ge sites per ethanelike unit, we must conclude that the concentration ratio of ethanelike Ge sites to CS tetrahedral Ge sites is 14.4 %. At this stage we must pause and reiterate that in Mössbauer spectroscopy one utilizes SnS$_2$ dopant to probe the structure of the GeS$_2$ glass. The simplest assumption is to say that Sn dopant randomly selects available Ge sites of the base glass. In the spectroscopy, one is unable to distinguish CS from ES tetrahedra. Fortunately in Raman scattering the ratio of A$_1$ to A$_1^c$ mode strength of 0.40(4) shows that there are 4 ES for every 10 CS tetrahedral in the structure. At 4.2 K, the Mössbauer I$_B$/I result of 17% or I$_B$/I$_A$ = 25% translates into a ratio of ethanelike units to CS units of

$25 \times (10/14) = 17.9\%$, which is in reasonable agreement with the matrix element corrected Raman scattering strength ratio of 14.4%.

For the C-nanophase, I_c/I (Mössbauer) =15%, or $I_C/I_A = 22\%$, translates into a ratio of rocksalt units to CS units of $22 \times (10/14) = 15.7\%$, and this ratio may be compared to the Raman mode scattering strength ratio of $A_c/A_1 = 2.90(5)\%$. These two results would be compatible if the Raman cross-section of the A_1 mode were fivefold larger than that of the 236 cm^{-1} modes. Unfortunately cross-section of the 236 cm^{-1} Raman modes is currently unavailable. The quantitative aspects of chemical order are better addressed by Mössbauer spectroscopy than Raman scattering because of these matrix element effects that are not easily decoded. The Mössbauer spectroscopy result obtained at 4.2K corrects for the recoil-free fraction changes between these sites [4], and provides a good representation of the concentration ratio of the octahedral to CS tetrahedral sites of 15.7% in GeS_2. The Raman results are generally consistent with not only the ^{119}Sn Mössbauer effect results presented here but also with earlier ^{129}I Mössbauer effect results[18] that show evidence of S-S bonds in GeS_2 glass. The latter contribute to Sn- mode at 494 cm^{-1} (Figure 3.13 (a)) and compensate for the presence of Ge-Ge bonds in the stoichiometric glass.

The absence of a compelling evidence for homopolar bonds in GeS_2 glass from neutron structure factors [8] can be understood. Given the concentration of ethanelike- and rocksalt units above, one arrives [9] at a concentration ratio of Ge-Ge to Ge-S bonds of 1.2% for GeS_2. The concentration of homopolar bonds anticipated for the

stoichiometric glass is at the limit of sensitivity of a diffraction measurement. These results highlight the much higher sensitivity of local probes (Raman scattering, Mössbauer spectroscopy) to ascertain the broken chemical order of a network by accessing sites or units of a network rather than counting the number of heteropolar versus homopolar bonds (as in a diffraction experiment).

4.2.2 Presence of Multiple nano-phases in GeS$_2$ and Trends in T$_g$

In recent years, compositional trends in T$_g$ in network glasses have been analyzed with remarkable success by stochastic agglomeration theory [10, 11]. The theory shows that within 10-15% latitude of bond-strengths, changes in T$_g$ intimately reflect those in network global connectivity. In our case the rapid increase of T$_g$ in S-rich glasses, particularly near x = 30.0, shows that all of the Ge additive serves to cross-link S$_n$-chains. The maximum in the slope dT$_g$/dx near x = 32.5, that precedes the maximum of T$_g$ near x = 33.33 (figure 3.11) underscores [10] that at x > 32.5, the additive preferentially nucleates structures (B and C units) that do not form part of the tetrahedral network, and lowers the global connectivity. In glass systems where T$_g$ continues to increase with cation concentration [12], such as the Si$_x$Se$_{1-x}$ binary, the Si-Si bonds formed at x > 33.33 form part of the backbone and melt viscosities increase astronomically. Taken together the Raman scattering, Mössbauer effect results, and trends in T$_g$ provide a rather complete picture of structure in the present glasses. They show that the stoichiometric glass is composed of a majority tetrahedral phase (A) in which minority nanophases (B and C) grow and break the chemical order and reduce the global connectivity of the network.

4.3 Molecular Structure of $(Ga_2S_3)_x$ $(GeS_2)_{1-x}$ Bulk Alloy Glasses

The structure of c-Ga_2S_3 has been described in two reports [13, 14] that are at variance with each other. In one report [13], the earlier of the two, the structure is viewed to be a defect wurtzite with $1/3^{rd}$ of the Ga sites unoccupied. In the other report, the structure is viewed to be octahedral [14]. Regardless, it is clear that in either structure the coordination of Ga is 4 or more and that of S is 3 or more. These coordination numbers are high for a glass to form. Constraint counting ideas [15] suggest that the additive will form a glass, if Ga is either 3 or 4-fold coordinated and S is 2-fold coordinated. In other words, the Ga : S ratio in the glass must nearly equal 1 : 2 or more.

These considerations suggest that for the additive (Ga_2S_3) to be incorporated in the GeS_2 base glass, additional S is required. Here we must remember that the Pauling electronegativity [16] of Ga (1.81), Ge (2.01) and S (2.58) makes it very likely that S will bond with Ga rather than Ge to optimize charge transfer effects. Such bonding will lower free energy of the alloyed glass network. We believe the GeS_2 base glass decomposes by reaction (8) to deliver S to the additive,

$$GeS_2 = Ge_2S_3 + S \tag{8}$$

The delivered S reacts with the additive (Ga_2S_3) to form GaS_2 by the following reaction,

$$Ga_2S_3 + S = 2\ GaS_2 \tag{9}$$

and the latter is incorporated in the Ge-rich glass as tetrahedrally coordinated $Ga(S_{1/2})_4$ local units. The alloying of $Ga(S_{1/2})_4$ units in the base glass in our model here leads Ge_2S_3 nanophase to form.

4.3.1 Low x Range (0 < x < 13%); Region I

In the low x range, formation of Ge-rich Ge_2S_3 nanophase dominates Raman scattering and $T_g(x)$ results. In Raman scattering, the growth in scattering of the 250 cm^{-1} band with Ga_2S_3 additive concentration x in the 0 < x < 17% range (Figure3.24a), supports the decomposition of the base glass by reaction (8) in the model above. A parallel behavior is observed [17,18] in Raman scattering of binary Ge_yS_{1-y} glasses at y > 1/3. The band is made up of two modes, one near 250 cm^{-1} and another near 236 cm^{-1}, that are identified respectively with normal vibrations of distorted rocksaltlike GeS and ethane like Ge_2S_3 units as discussed [17] recently.

Deconvolution of the Raman lineshapes of $(Ga_2S_3)_xGeS_2)_{1-x}$ glasses reveal that the average frequency of the 340 cm^{-1} band systematically upshifts (blue-shifts) from 343 cm^{-1} to 345 cm^{-1} as a function of x in the 0 < x < 17% range in figure 4.4. Our interpretation of the behavior is at present not clear. The vibrational mode frequency of trigonally distorted $Ge(S_{1/2})_4$ tetrahedral needs to be firmly established. Ga has 3 valence electrons $(3s^23p^1)$ tetrahedral coordination of Ga with S nearest neighbors may be possible if Ga forms 3 covalent bonds with S nns and a 4th dative bond. In the latter s donates an electron to the vacant Ga 3p orbital. And it is possible that the dative bond

may be slightly larger than the 3 covalent bonds. If this is case, the Ga local structure may be a trigonally distorted GaS4 rather than a perfect tetrahedral. The present results would suggest that this frequency ν (GaS$_4$) slightly exceeds ν (GeS$_4$). Ga EXAFS measurements [19] on these glasses studied at x = 0.15, 0.20 and 0.25 show Ga is 4-fold coordinated to 4s.
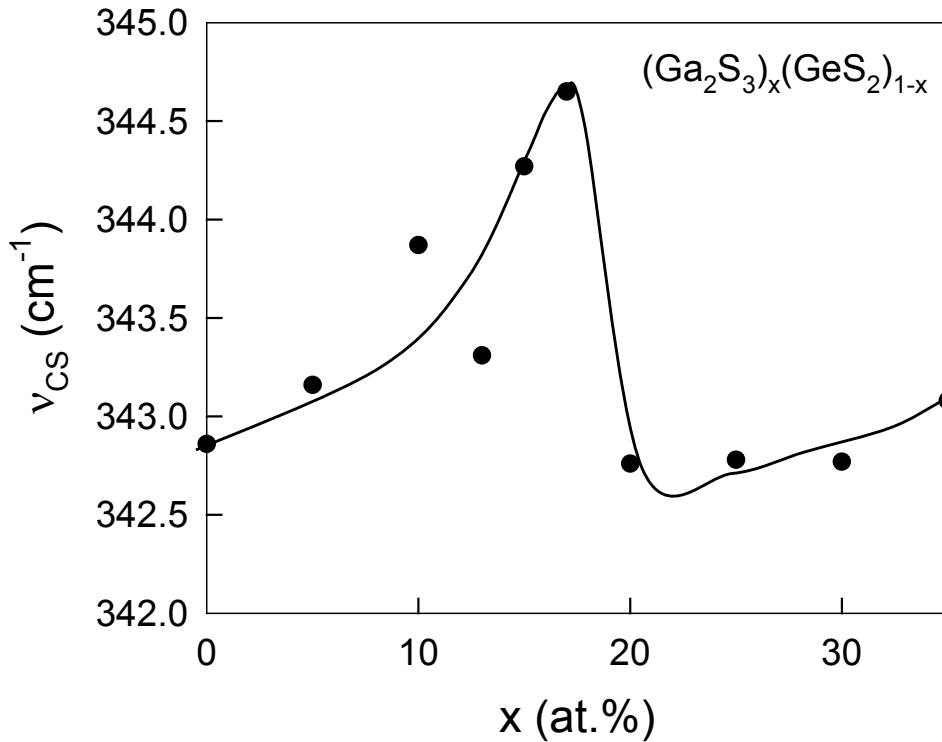
Figure 4.4 A$_1$ mode frequency of CS as a function of Ga$_2$S$_3$ composition x in GeS$_2$ Glasses.

The growth of the Ge-rich nanophase (Ge$_2$S$_3$ reaction 8) in our model of these glassy alloys above lowers their optical band gap in much the same fashion as reported[19] in binary Ge$_y$S$_{1-y}$ glasses at y > 1/3. Indeed, the remarkable change in color from yellow to dark brown as x increases to 17% can thus be understood in a natural way in our

model. The reduction in T_g of the present ternary parallels that of the Ge_xS_{1-y} binary as y>1/3, and arises due to a loss in network connectedness due to NSPS of Ge_2S_3 phase.

In summary, in the low x range, the physical picture of these alloy glasses suggested by our Raman and MDSC measurements is as follows. Ga_2S_3 additive largely enters the base GeS_2 glass as tetrahedrally coordinated $Ga(S_{1/2})_4$ units. The latter is facilitated by decomposition of the base glass to release S. The reduction in $T_g(x)$ in the same composition range is due to the fact that the global connectivity of the alloy glasses is lowered due to the formation of the Ge-rich (Ge_2S_3) nanophase as a byproduct of S release. The reduction in $T_g(x)$ in this range compares well to that in binary Ge_yS_{1-y} glasses in the Ge-rich region (y > 1/3).

4.3.2. Medium x Range (0.13 < x < 0.20); Region II

Compositional trends in $T_g(x)$ (Figure 3.22)and Raman lineshapes(Figure 3.24b) in region II are *not* a smooth extrapolation of results in region I , but in fact show quite a reversal of trends as can be seen in Figures 3.22, 3.24 b and 3.26 once x increases to 17%. All these results are suggestive of a threshold behavior near 17% that has structure manifestations. These results are suggestive of a qualitative change in molecular structure once x exceeds 13% in the alloy glasses. In region II the color of sample turns sharply dark brown in the near x = 17% which reverses itself as x increase to 20% and samples turn yellow again. The results in the 13% < x < 17% range mirror those in the 17% < x < 20% range as Ga_2S_3 is alloyed.

As the concentration of the Ga_2S_3 additive, x, exceeds 17%, it appears that the additive no longer *homogeneously* distributes in the base glass. We speculate that at the x > 17% the additive begins to segregate into a Ga-rich GaS nanophase,

$$Ga_2S_3 \ = \ 2\,GaS \ + \ S \tag{10}$$

to release S. The released S recombines to become GeS_2 like that now forms part of the backbone. Here the GaS nanophase is modeled after crystalline GaS [13] that consists of a layered structure in which Ga cations possess a heavily distorted rocksalt structure. The local coordination in the structure is thought to consist of 3 short and 3 long bonds. In region II, the sample color changes back to yellow as the optical gap of the alloyed glass increase. The latter is due to removed of the low gap Ge_2S_3 nanophase by connecting to GeS_2.

In Raman scattering one observes growth a new band centered near 462 cm^{-1} (labeled C') once x > 17% that we tentatively identify with the GaS nanophase. Here it would be pertinent to mention that the Ga_2S_3 nanophase in analogy to the Ge_2S_3 nanophase appears not to be stable with the more electropositive Ga cation. The same conclusion was reached by K.A.Jackson when he attempted to calculate the normal modes of a Ga_2S_3 cluster in which Ga has 4 nearest neighbors: one Ga and 3 S atoms. The ethanelike cluster is chemically unstable and breaks into two $Ga(S_{1/2})_3$ pyramids.

In Raman scattering, results of Figure 4.4 we note that the A_1 band frequency sharply downshifts in the narrow range17% < x < 20% range, and then remains constant in the 20% < x < 35% range (region III). The result suggests that much of the Ga that had entered the base glass in a tetrahedral local environment has rapidly leached out in the 17% < x < 20% range to attach itself in the GaS nanophase. The constancy of the A_1 band frequency (at 343 cm^{-1}) at x > 20% suggests that almost all of the Ga that was alloyed terahedrally in the base glass network has come out and attached itself to the Ga-rich GaS nanophase.

In summary, region II marks a transition region in which glass structure changes remarkably over a narrow composition range. In the lower half of region II the additive is largely alloyed in the base glass while in the upper half of the region II the additive segregates into a Ga-rich nanophase. These structural changes produce remarkable changes in the optical band gap of the glasses that is reflected in sample in color. The global minimum in T_g(x = 17%) reflects the largest concentration of the Ge-rich Ge_2S_3 nanophase. This phase has a lower connectivity than the terahedrally coordinated Ga- and Ge-bearing backbone because of the presence of redundant constraints[20]. The global minimum in T_g and band gap results from these aspects of molecular structure.

4.3.3. High x Range (0.20 < x < 0.35); Region III

76

In region III, Raman scattering reveals the growth of a band centered near 262 cm^{-1} labelled as C'. The scattering strengths of the A, B , C and C' bands is plotted in Fig. 3.26. Here we find that A, B and C bands characteristic base glass recover their scattering strength to values characteristic in region I, while the strength of the C' band increases monotonically with x. The latter result we identify with growth of the GaS nanophase as discussed above in section 4.3.2.

The DSC results of Loireau-Lazach have shown the existence of multiple crystallization events (T_x^1, T_x^2 and T_x^3) for glasses once x exceeds 0.25 but only one crystallization exotherm (T_x^1) at x < 0.25 in the present ternary glasses. These DSC results are in harmony of our proposal of NSPS of glasses at x > 0.25. At x < 0.25, crystallization entails formation of c-GeS$_2$. The melting point of c-Ga$_2$S$_3$ is high (1250 ^{o}C) and so it is likely that the Ga-rich phase never crystallizes and remains in an amorphous phase as glasses are heated to T > T_x^1. On the other hand, at compositions x > 0.25, multiple crystallizations are observed due to the formation of c-GeS$_2$, c-GaS and probably c-GeS. These speculations can be confirmed by additional x-ray diffraction measurements of glass samples heated past different stages of crystallization.

In summary, in region III, our Raman scattering and MDSC results suggest that the ternary glasses possess at leat two phases, a GeS$_2$ rich base glass phase and a GaS-rich nanophase. And it is likely that addition of Rare-earth additives in these ternary glasses leads the trivalent rare-earth atoms to replace trivalent Ga in the GaS nanophase.

REFERENCES:

1. Sudha Mahadevan and A. Giridhar, J. Non. Cryst Solids **152** (1993),42.

2. P. Boolchand and W.J. Bresser, Phil. Mag. B**80** (2000),1757.

3. A. Giridhar and Sudha Mahadevan, J. Non. Cryst Solids **151** (1992),245.

4. P. Boolchand**,** D.G.Georgiev, T. Qu, F. Wang, L.Cai, S.Chakravarty**.** Comptes Rendus Chimie **5** (2002), 713.

5. J.C. Phillips, Bonds and Bands in Semiconductors (New York Academic press, 1973), p22.

6. Jackson, A. Briley, S. Grossman, D.V. Porezag and M.R. Pederson, Phys. Rev. B**60** (1999), R14985.

7. G.Lucovsky,R.J.Nemanich, F.L.Galeener in *Proceedings of the 7th International Conference on Amorphous and Liquid Semiconductors,Edinburgh, Scotland*, 1977, Ed. W.E.Spear(G.G.Stevenson, Dundee, Scotland, 1977), p.130

8. W.J. Bresser, P. Boolchand, P. Suranyi, J.P. deNeufville, Phys. Rev. Lett. **46**(1981), 1689; H.R. Chandrasekhar, R.G. Humphreys, U. Zwick, M. Cardona, Phys. Rev. B**15** (1977),2 177 and references therein.

9. In a GeS$_2$ network, for every 100 CS units, we have 40 ES ones, 15 distorted rocksalt ones, and 8.8 ethanelike units. The bond fraction, N_{Ge-Ge}/N_{Ge-S} =8.8/[(100 x 4) + (40 x 4) + (15x 6) + (8.8 x 6)] =1.2%.

10. M. Micoulaut and G.G. Naumis, Europhysics Letters **47** (1999), 568.

11. R. Kerner and M. Micoulaut, J. Non Cryst Solids **210** (1997), 298.

12. D.Selvanathan, W.J. Bresser and P.Boolchand, Phys. Rev B **61** (2000),15061. Also see J.E Griffiths, M. Malyj, G.P. Espinosa and J.P. Remeika, Phys. Rev. B **30**

(1984), 6978.

13. J. Goodyear and G.A. Stelgmann, Acta Cryst. **16** (1946), 946.

14. J. Goodyear, W.J. Duffin and G. A. Steigmann, Acta Cryst. **14** (1961), 1168**.**

15. J. C. Phillips**,** J. Non Cryst Solids **34** (1997), 153.

16. L.Pauling, Nature of the Chemical Bond, Cornell University Press, 1960, p.93.

17. Liuchun Cai and P. Boolchand, Phil. Mag. B **82** (2002),1649.

18. P. Boolchand, J. Grothaus, M. Tenhover, M.A. Hazle and Robert K. Grasselli, Phys. Rev. B **33** (1986), 5421.

19. A.M. Loireau-Lozach, J. Sol. Stat. Chem. **123** (1996), 60.

20. J. M. Saiter, J. Ledru, G. Saffarini and S. Benazeth, Materials Letter **28** (1996), 451.

21. J. M. Saiter, J. Ledru, G. Saffarini and S. Benazeth, Materiasl Letter **35** (1998), 309.

22. S. Mahadevan and A. Giridhar, J. Non Cryst Solids **143** (1992), 52.

23. U. Tille, G. H. Frischat and K. J. Leers, J. Non-Crystalline Solids, (1977), 631.

24. S. Blaineau and Philippe Jund and D. Drabold, Phy. Rev. B **67** (2003), 094204.

Chapter 5

CONCLUSIONS

The principal conclusions of the present work are as follows.

1. Doping Behavior of Group III Additive "In" in Base Ge_xSe_{1-x} Glasses. MDSC results show that variations in glass transition temperatures, $(dT_g/dy)_{obs}$, in $Ge_xIn_ySe_{1-x-y}$ glasses as a function of In doping 'y' yield slopes that quantatively match the predicted slopes $(dT_g/dy)_{pred}$ based on a model in which the additive segregates into nanocrystalline In_2Se_3 clusters. A parallel behavior is suggested for Ga as an additive in Ge_xSe_{1-x} glasses at x >0.26.

2. Molecular structure of Stoichiometric GeS_2 Glass. Raman scattering, MDSC and Mössbauer spectroscopy results show that the stoichiometric GeS_2 glass ($T_g = 508°C$) is partially polymerized into 3 phases; a majority phase consisting of $Ge(S_{1/2})_4$ tetrahedra (A); Ge-rich minority phase consisting of ethanelike $Ge_2(S_{1/2})_6$ units (B), and a minority GeS phase consisting of distorted rocksalt $Ge(S_{1/6})_6$ units(C) in approximately 93.4 : 3.6 : 3.0 ratio. Parallel results of nanoscale phase separation are suggested by [119]Sn Mössbauer spectroscopy.

3. Evolution of Glass Structure in the $(Ga_2S_3)_x(GeS_2)_{1-x}$ Ternary as a Function of Ga_2S_3 Additive. Raman Scattering and T-modulated DSC show that the molecular

structure of $(GeS_2)_x(Ga_2S_3)_{1-x}$ glasses display a rather striking anomaly near x = 17%. In the $0 < x < 17\%$ range, the additive (Ga_2S_3) enters the base glass as $Ga(S_{1/2})_4$ units forming part of the base glass network, which results in Ge-rich Ge_2S_3 units to segregate from the backbone. At x > 17%, the additive (Ga_2S_3) nucleates a Ga-rich, GaS like phase, releasing S that permits Ge_2S_3 nanophase to alloy back in the base glass network. These molecular structure results provide a basis to understand the global minimum in the band gap and T_gs of these ternary glasses reported in this work for the first time.

Appendix A

Raman Scattering Results of Indium as an Additive in Ge_xSe_{1-x} Glasses

Figure A-1 and A-2 display the evolution of the Raman line shapes with In content in ternary $Ge_{10}In_ySe_{90-y}$ and $Ge_{22}In_ySe_{78-y}$ glasses. The modes at 200, 215, 250 cm^{-1} have been previously identified with corner-sharing (CS), edge-sharing (ES) $Ge(Se_{1/2})_4$ tetrahedra and Se_n chains, respectively. Noteworthy in these scans is the systematic reduction in the scattering strength of the Se_n-chain mode (CM) with In alloying. One can infer In_2Se_3 presence by depletion of the Se_n CM.

Figure A-3 (a) and (b) provides a plot of the observed scattering strength of the CM (A^{cm}) normalized to sum of the CS mode (A^{cs}) and ES mode (A^{es}) as a function of y. The results show that the depletion rates $d(A^{cm}/(A^{cs} + A^{es})/dy$ in the $Ge_{10}In_ySe_{90-y}$ and $Ge_{22}In_ySe_{78-y}$ are 0.07 and 0.044. The reduction in these ratios with y is currently being modeled to understood these observation
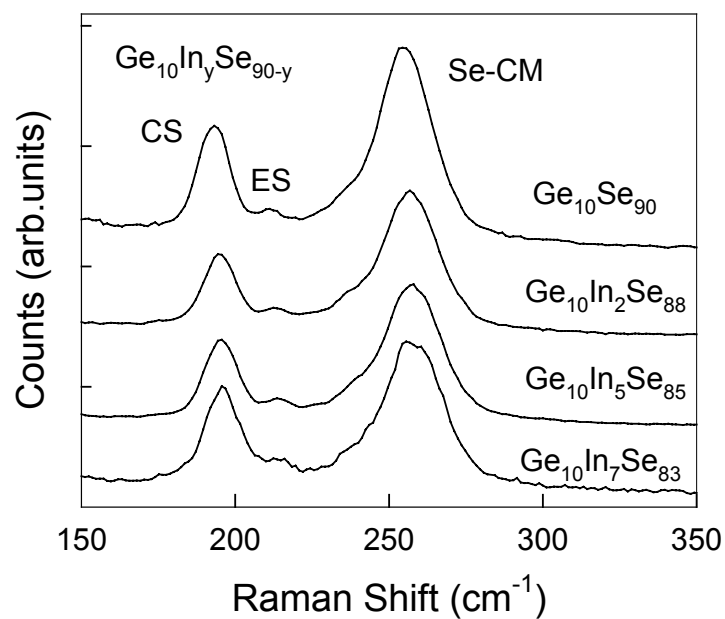
A-1 Raman scattering $Ge_{10}In_ySe_{90-y}$ ternary glasses showing depletion of the Se_n chain mode with In content. The chain mode (CM), corner-sharing (CS) and edge-sharing (ES) are indicated.
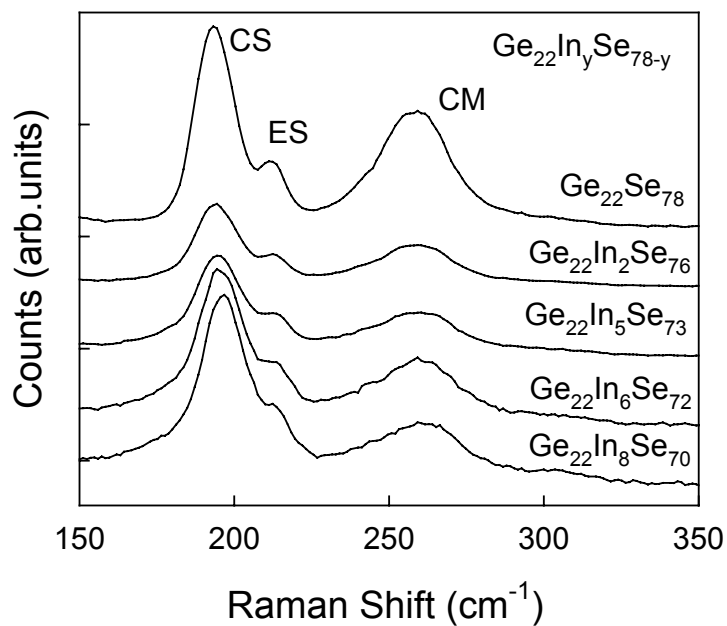
A-2 Raman scattering $Ge_{22}In_ySe_{78-y}$ ternary glasses showing depletion of the Se_n chain mode with In content.
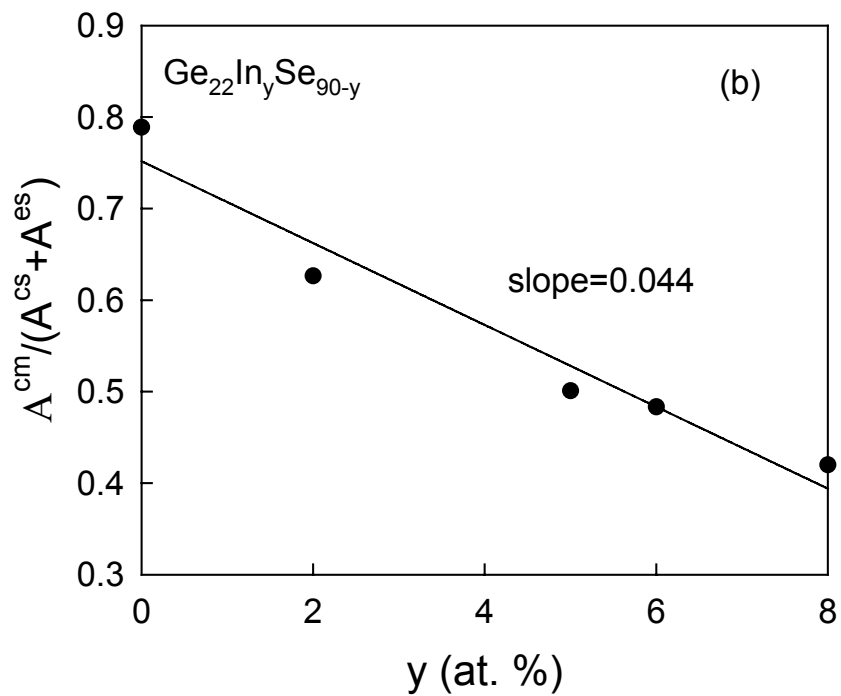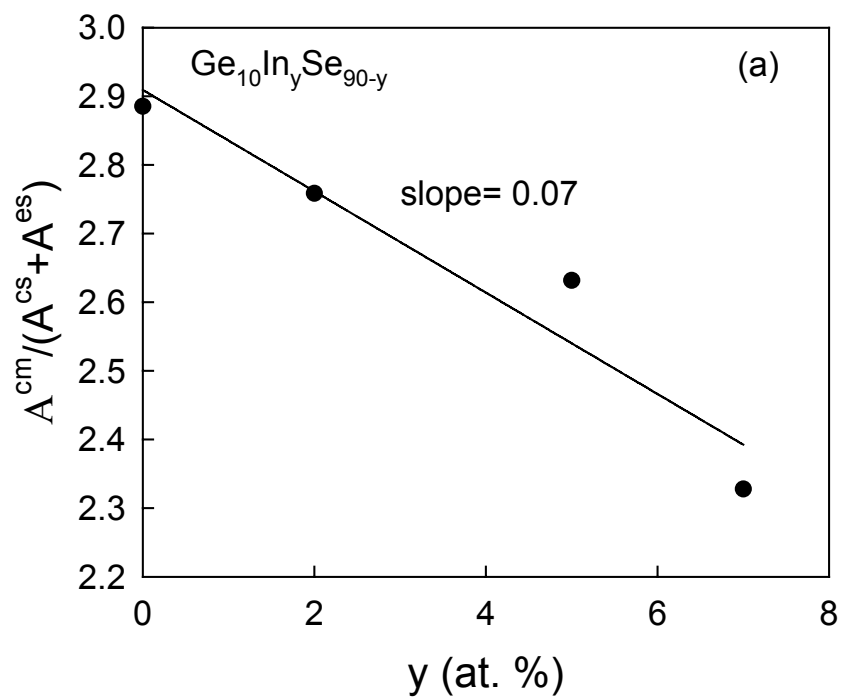
A-3 (a) and (b) Se_n-Chain mode scattering strength variation normalized to sum of CS mode and ES mode in the ternary glasses $Ge_{10}In_ySe_{90-y}$ and $Ge_{22}In_ySe_{78-y}$, respectively.